19

Inherited Upper-Plate Controls on Localized Arc Magmatism Since ca. 100 Ma Along the Alaska Range Suture Zone

Jeffrey A. Benowitz[1] and Michael Everett Mann[2]

ABSTRACT

Long-lived continental magmatic arcs may migrate large (hundreds of kilometers) trench perpendicular distances as convergent margin configurations and slab geometry vary over time; however, many arc-magmatic belts are spatially localized over tens of millions of years. We document, by compiling published crystallization geochronology data for southern Alaska (6,485 total bedrock and single-grain detrital ages combined), that since ca. 100 Ma, arc magmatism has been localized along the Alaska Range suture zone (in places within a 10 km × 5 km swath) and at times over 500 km inboard. However, since ca. 100 Ma, incoming subducting slab characteristics and convergent margin configurations varied greatly and include both normal oceanic plate and oceanic plateau subduction, plate vector changes, oroclinal bending and reconfiguration of trench shape, terrane accretion, long-distance terrane translation, and a Paleocene slab break off/slab window event. Therefore, it is inferred that inherited upper-plate lithospheric thickness and thermal variations must control in part the geometry of the subducting slab below a mobile southern Alaskan margin through hydrodynamic mantle wedge "suction" forces. Additionally, crustal thickness heterogeneity may focus magma ascent through melt ponding along Moho offsets, and upper-plate lithospheric-scale strike-slip faults may be acting as passive and active conduits for arc magmatism.

19.1. INTRODUCTION

The upper-plate location of continental arc magmatism is broadly correlated with the geometry of the subducting slab, with melt generation and individual volcanic centers generally positioned above the subducting slab 130 ± 70 km depth contours (England et al., 2004; Isacks & Barazangi, 1977; Syracuse & Abers, 2006; van Keken et al., 2011). Numerous factors can influence subducting slab geometry, including the age of the incoming slab (Jarrard, 1986), buoyant topographic highs (e.g., oceanic plateaus: Van Hunen et al., 2002, 2004; aseismic ridges: George et al., 2022), the thickness of the overriding plate (e.g., Sharples et al., 2014), trench shape and curvature (e.g., Chiao et al., 2002), convergence rate (e.g., Billen & Hirth, 2007), and convergence obliquity (e.g., Laurencin et al., 2018). Thus, overall continental arc localization should be limited, given the dynamic nature of long-lived subduction systems, wherein slabs can break off and active ridges can subduct, the age of the incoming plate can change over time (Grow & Atwater, 1970), incoming plate speed and direction can both vary with time (Richards & Lithgow-Bertelloni, 1996; Stock & Molnar, 1988), and bathymetric highs can be fully subducted (Gutscher et al., 1999) or accreted (Yang et al., 2015). Thus, it is generally accepted that long-lived continental arcs should migrate large trench perpendicular distances

[1] *Department of Geological Sciences, University of Boulder, Boulder, CO, USA*

[2] *Department of Earth, Environmental and Planetary Sciences, Brown University, Providence, RI, USA*

Tectonics and Seismic Structure of Alaska and Northwestern Canada: EarthScope and Beyond, Geophysical Monograph 290, First Edition.
Edited by Natalia A. Ruppert, Margarete A. Jadamec, and Jeffrey T. Freymueller.

DOI: 10.1002/9781394195947.ch19
Companion website: www.wiley.com/go/Ruppert

as both slab and upper-plate geometries morph over time (Chapman & Ducea, 2019; Kay et al., 2005; e.g., Gianni & Luján, 2021).

Hence, how continental arcs can be localized on 10^7-year timescales (Farrar et al., 2023; Humphreys & Grunder, 2022; Kirsch et al., 2016; Ma et al., 2022; Rabiee et al., 2020), hundreds of kilometers inboard of a nonstationary trench remains an enigma. Furthermore, during periods of strike-slip activity, crustal blocks along strike-slip faults are translated to new positions, intrinsically creating a possible unclear geological record of arc localization (Alvarado et al., 2016; Trop et al., 2022). Moreover, overriding plates themselves are always in relative motion to the incoming slab (DeMets et al., 2015), and trench-to-arc distance can also vary with time due to accretion (Hughes & Pilatasig, 2002) and subduction erosion (Stern, 2011). Potential arc localization is compounded further by the fact that fluids and hence melt can be generated from a large area of a shallow dipping subducting slab mantle wedge interface (Arce et al., 2020) and channeled updip (Cagnioncle et al., 2007; Hicks et al., 2023; Wilson et al., 2014).

In this work, we document arc-localization inboard of the proto and modern Pacific trench along the mobile Alaska Range suture sone (*ARSZ*; Brennan et al., 2011; Box et al., 2019; Ridgway et al., 2002; Trop et al., 2019) since ca. 100 Ma (Figure 19.1). Variability of incoming subducting slab characteristics and convergent margin configurations—including both normal oceanic plate and oceanic plateau subduction (e.g., Jones III et al., 2021), plate vector changes (Doubrovine & Tarduno, 2008), oroclinal bending (e.g., Gillis et al., 2022) and reconfiguration of trench shape (e.g., Mann et al., 2024), terrane accretion (e.g., Trop & Ridgway, 2007), and a Paleocene slab break off/slab window event (Benowitz et al., 2012; Terhune et al., 2019)—have not drastically affected *ARSZ* arc location with time. Nor has long distance translation of the ARSZ along the western margin of North America

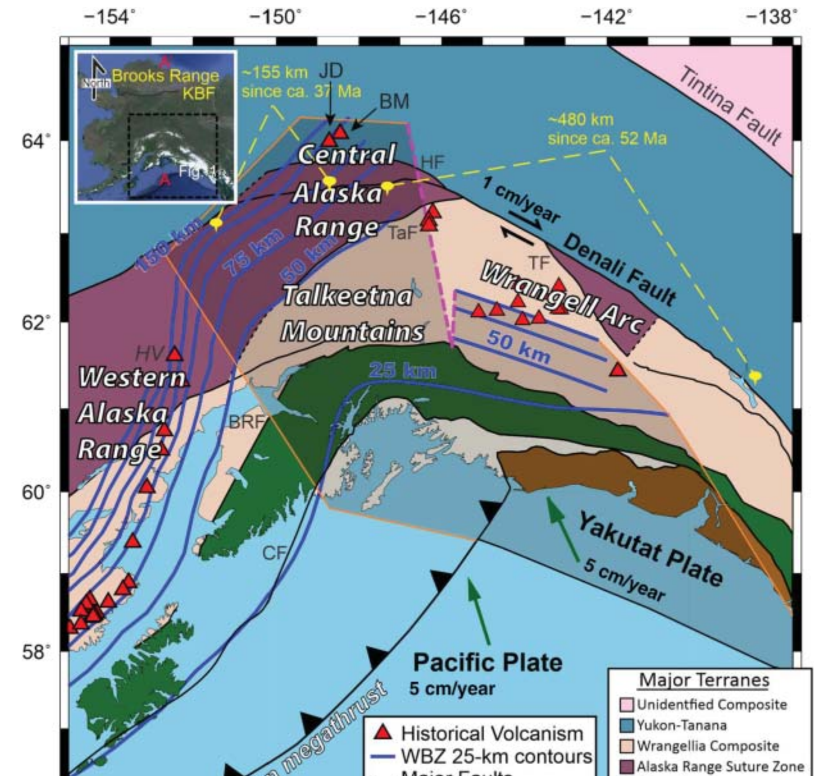

Figure 19.1 Modern configuration of the subducting slab and major terranes across southern Alaska. JD, Jumbo Dome; BM, Buzzard Maar; HV, Hayes Volcano; CF, Contact Fault; BRF, Border Ranges Fault; TaF, Talkeetna Fault; TF, Totschunda Fault; HF, Hines Creek Fault; KBF, Kobuk Fault. Blue lines are 25 km contours of subducting slab (Mann et al., 2022). The gray polygon is an outline of the seismically imaged Yakutat terrane (Mann et al., 2022). Historical volcanos are from Cameron (2005). Denali and Totschunda faults' displacement history is from Regan et al. (2021), Waldien et al. (2021), and Rosenthal et al. (2024). Terrane locations are simplified from Colpron and Nelson (2011). A and A′, location of Figure 19.2 cross-section.

(>2,000 km; e.g., Stamatakos et al., 2001; Tikoff et al., 2023). These observations suggest that previous models may have overlooked the important effects of the inherited upper-plate lithospheric thickness and temperature contrasts across the *ARSZ* and northern Alaska (Gama et al., 2022; Miller et al., 2018) and along the western-Northern Cordillera (Clowes et al., 1995; Estève et al., 2020) on the subducting slab geometry under the Wrangellia composite terrane of southern Alaska. We suggest arc localization, since ca. 100 Ma, has been in part controlled by upper-plate-related hydrodynamic (viscous) slab mantle wedge interface "suction" forces, melt ponding at Moho offsets, and upper-plate lithospheric-scale strike-slip faults acting as passive and active conduits for arc magmatism (Figure 19.2).

19.2. GEOLOGIC BACKGROUND

19.2.1. Jurassic to Recent Southern Alaska Convergent Margin Tectonics

Southern Alaska has been a convergent margin since at least the Triassic (Kusky et al., 2007; Trop & Ridgway, 2007), with periods of (1) accretionary events (e.g., Jura-Cretaceous: Trop et al., 2020; Eocene: Garver & Davidson, 2015), (2) oroclinal bending changing the orientation and shape of the plate margin (e.g., Gillis et al., 2022), (3) slab-window/transform tectonics with a gap in arc magmatism (ca. 60–50 Ma; Terhune et al., 2019), (4) periods of "normal" subduction (Kula slab: ca. 100–60; Pacific slab: 45–30 Ma; Benowitz et al., 2022a; Jones III et al., 2021; Terhune et al., 2019; Trop et al., 2019), and (5) flat/shallow slab subduction of the Yakutat oceanic plateau with initiation of the associated slab-edge Wrangell Arc (30 Ma to Recent; Berkelhammer et al., 2019; Brueseke et al., 2019, 2023a; Ebherhart-Phillips et al., 2006; Jadamec, 2016; Trop et al., 2022; Worthington et al., 2012).

The accretion of the Wrangellia composite terrane to North American affinity crust was the largest addition of crust to the continent in the last 150 million years (Trop & Ridgway, 2007). The generally accepted model is that the Wrangellia composite terrane, primarily thick oceanic plateau crust, collided along and in places may have subducted under North America's western coast at around ca. 100 Ma (Trop & Ridgway, 2007) and then was translated >2,000 km north along margin-parallel strike-slip fault systems (e.g., Tikoff et al., 2023). The *ARSZ* (Ridgway et al., 2002) is the suture region and closed oceanic basin between the Wrangellia terrane and rocks of North American affinity to the north (Figure 19.1). The lithospheric-scale Denali Fault system delineates the northern boundary of the *ARSZ* (Fitzgerald et al., 2014; Newell et al., 2023; Trop et al., 2019, 2022), with the Talkeetna Fault delineating the southwestern and Totschunda Fault delineating the southeastern boundaries of the *ARSZ* (Allam et al., 2017; Brennan et al., 2011) with the Kahiltna Mesozoic marine assemblage and equivalents in between (Box et al., 2019; Manselle et al., 2020; Ridgway et al., 2002; Trop et al., 2020). By ca. 50 Ma, the Chugach-Prince William Terrane had been translated and accreted into place south of the Border Ranges Fault system of southern Alaska (Figure 19.1) (Garver & Davidson, 2015).

Crustal thickness varies across the Border Ranges Fault system (Mann et al., 2022), the Talkeetna Fault (Brennan et al., 2011), and the Denali Fault system (Allam et al., 2017) with clear magnetic contrasts across all three structures (Saltus & Hudson, 2022). The Moho offset across the Denali Fault system is ~10 km with the crust thinner to the north of the fault (Allam et al., 2017; Mann et al., 2022; Rossi et al., 2006; Veenstra et al., 2006; Yang et al., 2024). The Denali Fault also has a well-defined across-strike lithosphere thickness variation: the lithosphere is at least 15 km thicker and is colder to the north of the Denali Fault (>65 km) compared to the south (Gama et al., 2022; Miller et al., 2018) based on seismic velocity analysis. The Arctic Plate (Brooks Range) north of the Kobuk Fault (Figures 19.1 and 19.2) has an even thicker crust (>45 km; Miller et al., 2018; Yang et al., 2024) and an apparently cratonic (McClelland et al., 2021) thick (~200 km) and cold lithosphere (Gama et al., 2022; Jiang et al., 2018; O'Driscoll & Miller, 2015; Pavlis et al., 2024). These crust and lithospheric variations are primarily inherited (i.e., older than ca. 100 Ma) with some post docking shortening along the *ARSZ* (Ridgway et al., 2002) and Eocene extension south of the Hines Creek Fault (Gillis et al., 2022). Notwithstanding these tectonic events, the overall trend of thinner-hotter lithosphere to the south and progressively thicker-colder lithosphere inboard has been a long-lived feature (O'Driscoll & Miller, 2015).

The modern plate configuration includes the Yakutat slab that has a shallow dip of ~5° for nearly 200 km inboard of the trench and is in direct contact with the overriding crust until it reaches the Chugach-Prince William Terrane–Wrangellia composite terrane boundary (Kim et al., 2014; Mann et al., 2022). Once the subducting slab reaches roughly the Talkeetna Fault, its dip increases gradually to ~20° (Ferris et al., 2003; Rondenay et al., 2010); near the Denali Fault it begins steeply dipping into the mantle (Jiang et al., 2018; Yang et al., 2024). Flat slab subduction of the Yakutat microplate (Figure 19.1), an oceanic plateau, is currently linked to its inferred buoyant and seismically imaged thick crust (~11 km to ~30 km) (e.g., Christeson et al., 2010; Rondenay et al., 2010; Worthington et al., 2012).

19.2.2. Mobility of the System and Varying Age of the Subducting Slab

The exact location of the paleosouthern Alaska trench is not known, but we assume that the trench was near the Border Ranges Fault transform system ca. 100 Ma till ca. 50 Ma (Terhune et al., 2019) because there is an imaged paleo-subduction zone interface along this structure (Mann et al., 2024) and then jumped out closer to its modern position after the accretion of the Chugach-Prince William Terrane (Garver & Davidson, 2015), with additional trench modifications with the arrival of the Yakutat Terrane (e.g., ca. 30 Ma; Brueseke et al., 2019) (Figure 19.1). Southern Alaska is also bisected by three major dextral strike-slip fault systems. The Tintina Fault has seen ~490 km of displacement, primarily during the Eocene (Saltus et al., 2007). The Denali Fault system has experienced at least ~480 km of displacement since ca. 52 Ma (Figure 19.1) (Rosenthal et al., 2024; Waldien et al., 2021). The Border Ranges Fault system has experienced at least ~700 km of offset between ca. 58 Ma and 50 Ma (Smart et al., 1996). More speculatively the Teslin Fault system (not shown in Figure 19.1) of the Yukon Territory may have experienced 1,900 km of displacement since ca. 70 Ma (Johnston et al., 1996). Thus, the paleolatitudinal location of the *ARSZ* has varied with time and hence the region's relative position to stable North America. Furthermore, North America/Alaska was ~10° further to the north during the late Cretaceous as compared to today (e.g., Tikoff et al., 2023) and North America continues to move southwest relative to the Pacific Plate (Anders, 1994; DeMets & Dixon, 1999), which likely led to trench encroachment of the inboard regions (i.e., cratons) of thick lithosphere (Figure 19.2).

Since ca. 84 Ma, there have been at least five significant proto-Pacific and Pacific Northeast plate motion changes. Based on Doubrovine and Tarduno (2008), at 84 Ma proto-Pacific and Pacific Northeast slab movement had an orientation of ~356° NE, then at 67 Ma orientation rotated 14° counterclockwise, then at 62 Ma rotated 11° clockwise, and then at 50 Ma rotated 16° clockwise. At 25 Ma, there was an 8°–15° counterclockwise rotation (Jicha et al., 2018) and an 18° clockwise rotation at ca. 6 Ma of the Pacific slab (Austermann et al., 2011; Engebretson et al., 1984). The rate of convergence has also varied, with rates from 50 to 200 km/Ma during the last 84 My (Doubrovine & Tarduno, 2008; Elliott et al., 2010). The age and therefore temperature and thickness of the subducting slab under the Wrangellia composite terrane has clearly varied through time, but determining the age of ancient subducted slabs is not always feasible as all previous slab material has descended into the mantle. At 50 Ma, the age of the subducting Pacific slab under Alaska was likely young given subduction had reinitiated after the break-off of the Kula Plate (e.g., Terhune et al., 2019). Furthermore, the majority of the currently subducting Yakutat slab formed ca. 50 million years ago (Wells et al., 2014).

19.3. METHODS

We compiled bedrock U-Pb zircon and detrital U-Pb zircon watershed populations across southern Alaska and combined them with known plate boundary constraints (subduction versus the presence of a slab window) to determine the spatial patterns of continental arc magmatism since ca. 100 Ma (Figures 19.3 and 19.4). We chose this age cutoff based on when large segments of the Wrangellia composite terrane would have interacted with the North American Plate (e.g., Tikoff

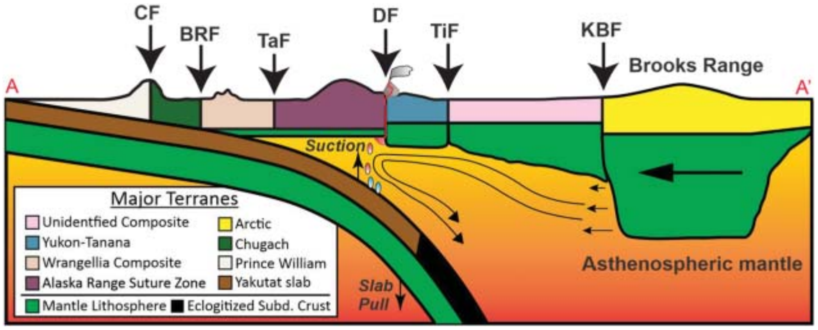

Figure 19.2 Schematic depiction of the current Alaska eastern subduction zone and interpretation of mantle flow. Resultant mantle-flow-related hydrodynamic "suction" in the mantle wedge relative to the trench encroaching craton, and Moho offsetting faults acting as magma conduits and regions of melt ponding. Thicknesses are approximate—see the text for references. Terrane locations are simplified from Colpron and Nelson (2011). Figure is not drafted to scale. CF, Contact Fault; BRF, Border Ranges Fault; TaF, Talkeetna Fault; TF, Totschunda Fault; DF, Denali Fault; TiF, Tintina Fault; KBF, Kobuk Fault.

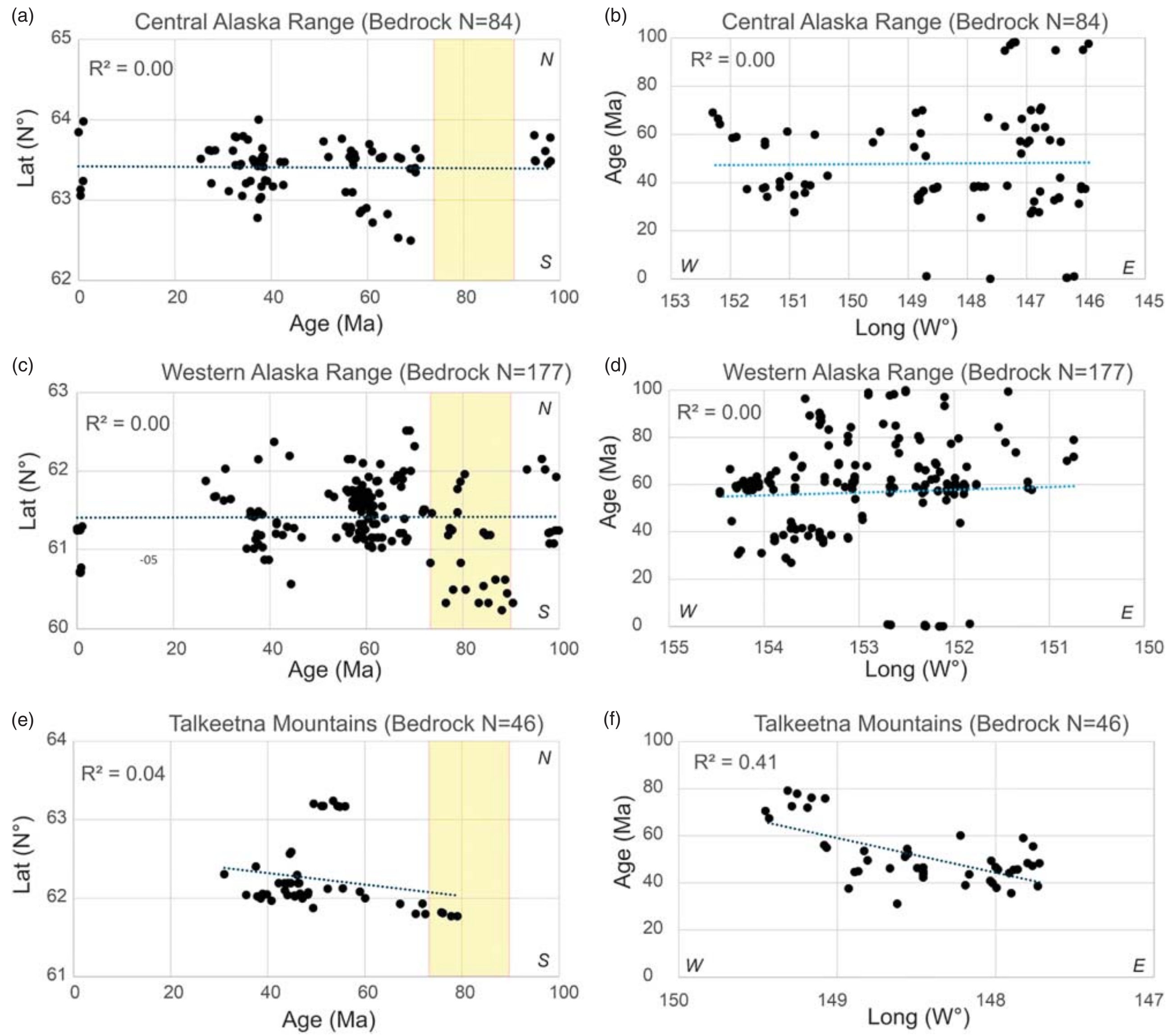

Figure 19.3 Latitude versus age and age versus longitude for bedrock samples <100 ca. Ma from the Western (a,b) and Central Alaska Range Arc (c,d) and the Talkeetna Mountains (e,f). Wrangell Arc is not shown because of a complicated history involving slab edge droop and dissection by the Totschunda Fault. See the text and Trop et al. (2022) for a detailed reconstruction of the Wrangell Arc spatial variation. Yellow swath highlights the shift in magmatism ca. 87 to 75 Ma to the south for the Western Alaska Range and the Talkeetna Mountains and the gap in magmatism in the Central Alaska Range. S, south; N, north; E, east; W, west. Blue dashed lines are linear least squares trend lines with R^2 value shown. Data are available in supporting information Tables S1–S4 on the companion website.

et al., 2023), but acknowledge that ocean-basin suturing was diachronous in both time and space (Trop et al., 2020; Waldien et al., 2021). We bolstered this data set with $^{40}Ar/^{39}Ar$ and K–Ar ages on mafic dikes and volcanics and detrital $^{40}Ar/^{39}Ar$ lithic grains. We did not compile $^{40}Ar/^{39}Ar$ and K–Ar ages on hornblende, muscovite, biotite, or potassium feldspar to avoid dates that reflect exhumation or metamorphic related events—not true magmatic events except from magmatic products from the relatively undeformed (<30 Ma) Wrangell Arc. We generally avoided ashfall samples because of unknown sources, but some thick welded tuffs are included in the data set. The detrital data sets may include some recycled grains from sedimentary or metamorphic lithologies (Wilson et al., 2015), but the detrital data sets mimic the igneous bedrock data sets, except for the Wrangell Arc region. The glaciated Wrangell Arc region has limited bedrock geochronology data;

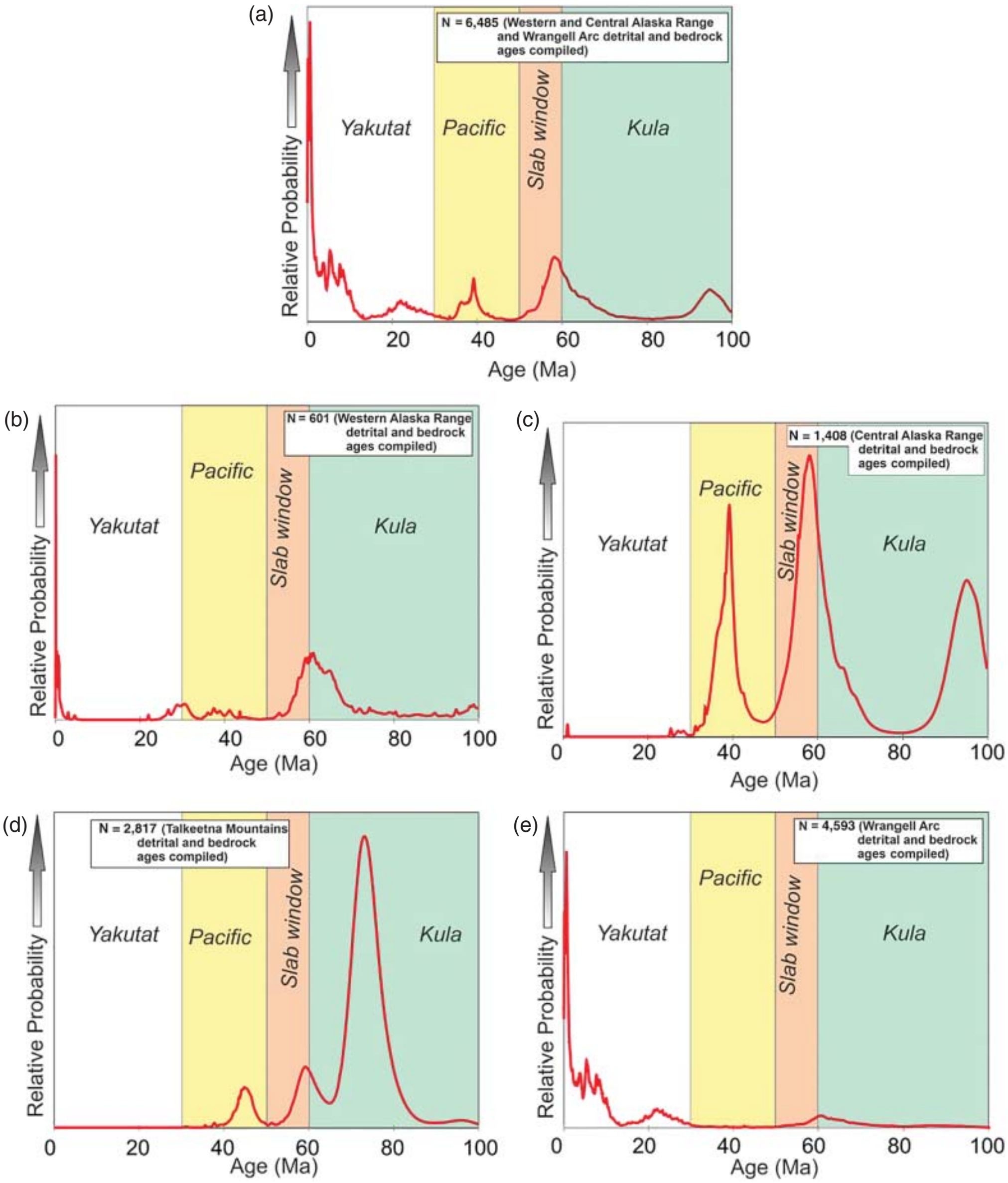

Figure 19.4 Probability density plots of compiled published bedrock ages and detrital single-grain ages <ca. 100 Ma from (a) the Western Alaska Range, Central Alaska Range, and the Wrangell Arc combined (*ARSZ* arcs), (b) the Western Alaska Range, (c) the Central Alaska Range, (d) the Talkeetna Mountains, and (e) the Wrangell Arc. Data are available in supporting information Tables S1–S4 on the companion website. Kula slab subduction period (100–60 Ma); slab window (60–50 Ma); Pacific slab dominated (50–30 Ma); Yakutat slab dominated (30 Ma to Recent). Note the Western and Central Alaska Range arcs have continued magmatism to ca. 25 Ma when magmatism ceased due to Yakutat flat slab subduction. The Western and Central Alaska Range arcs reinitiated at ca. 1 Ma coeval with the tearing and slab segmentation of the Yakutat slab (Brueseke et al., 2023b; Jones III et al., 2021; Trop et al., 2019). Plots made with isoplot, where the Y axis is unitless relative probability (Ludwig, 2012).

hence, the detrital data set captures additional magmatic events. For the purposes of this work, we refer to all magmatism near the ARSZ along the greater Totschunda Fault region as Wrangell Arc magmatism, distinct from the common nomenclature usage only applying to the last 30 million years of Yakutat slab related Wrangell Arc magmatism (Brueseke et al., 2019). We do not include detrital ages from Cretaceous–Cenozoic strata to avoid potentially far-traveled sources (Finzel, 2019).

Locations were all plotted and assumed to be in the geodetic datum, WGS84. For the purposes of this study, the potential 500–1,000 m difference from NAD27 is not germane, but we recommend attempting to figuring out (often not reported) the original datum applied, if using this compiled database for other purposes. Detrital geochronology data sets for individual watersheds from the Western and Central Alaska Range arcs and the Wrangell Arc are presented individually on the companion website, but compiled for figure presentation. The watershed outlines are presented in the references noted in the supplemental files. Data and further references are available in supporting information Tables S1–S4 on the companion website.

We overlayed our geochronology data set on a simplified terrane map of Alaska (Figure 19.5). Bedrock samples north and at the apex of the Denali Fault are shown at a higher spatial resolution in Figure 19.6 on the terrane map. To highlight arc localization, time slices were created for 100–60 Ma (Kula slab; e.g., Doubrovine & Tarduno, 2008), 60–50 Ma (slab window; e.g., Terhune et al., 2019), 50–30 Ma (Pacific; e.g., Trop et al., 2019), and 30 Ma to Recent (Yakutat slab; e.g., Brueseke et al., 2019) for the Western and Central Alaska Range arcs (northern continental Aleutian since ca. 48 Ma; Bezard et al., 2021) and the Talkeetna Mountains. For the Western and Central Alaska Range arcs, time slices are 100–60, 60–50, 50–25, and 25 Ma to recent to reflect the continuation of arc magmatism after the initial arrival of the Yakutat slab at ca. 30 Ma (Brueseke et al., 2019; Jones III et al., 2021; Trop et al., 2019). These divisions are based on known periods of arc magmatism, pulses of arc magmatism, and significant changes in plate boundary conditions as described in detail in the Geological Background section (Benowitz et al., 2022a: Fasulo & Ridgway, 2021; Finzel, 2019; Herriott, 2014; Jones III et al., 2021; Lease et al., 2016; Regan et al., 2020, 2021 Terhune et al., 2019; Trop et al., 2019, 2022). We also overlay bedrock and detrital data on a map of crustal thickness variations for 50–30 Ma and 30 Ma to Recent time slices (Figure 19.7) (Brennan et al., 2011; Regan et al., 2020, 2021; Miller et al., 2018; Veenstra et al., 2006; Yang et al., 2024). We do not use a lithospheric thickness map as a background because of the limited spatial coverage (e.g., Gama et al., 2022), but we compile lithospheric thickness constraints for each terrane for Figures 19.2 and 19.8 (Gama et al., 2022; Jiang et al., 2018; O'Driscoll & Miller, 2015).

19.4. RESULTS

19.4.1. Western Alaska Range Arc

We compiled 179 bedrock ages and 422 single-grain U-Pb zircon ages from the Western Alaska Range Arc (Figures 19.3–19.6; references in supporting information S1). The swath of arc magmatism along the Western Alaska Range Arc spans from ca. 100 to 25 Ma with re-initiation of the arc since ca. 1 Ma, based on the compilation of both bedrock and detrital geochronology data sets (Cameron et al., 2022; Herriott, 2014; Jones III et al., 2021; Lease et al., 2016). Periods of peak magmatism are ca. 98 Ma, 60 Ma, throughout the Oligocene, and since ca. 1 Ma (Figure 19.4). There are no substantial East–West or North–South trends with time besides (1) a jump trenchward in magmatism from ~87 to ~75 Ma (Figure 19.3) and (2) the modern Denali magmatic gap (Rondenay et al., 2010) between Hayes Volcano and Jumbo Dome-Buzzard Maar to the northeast (Figure 19.1).

19.4.2. Central Alaska Range Arc

We compiled 83 bedrock ages and 1,325 single-grain U-Pb zircon ages from the Central Alaska Range Arc (Figures 19.3–19.7; references in supporting information S2). The swath of arc magmatism along the *ARSZ* pulses from ca. 100 to 25 Ma, with re-initiation of the arc since ca. 1 Ma based on the compilation of both bedrock and detrital geochronology data sets (Andronikov & Mukasa, 2010; Athey et al., 2006; Benowitz et al., 2022a; Brueseke et al., 2023b; Fasulo & Ridgway, 2021; Lease et al., 2016; Regan et al., 2020, 2021) with a focus along the Denali Fault system. Overall, there is minimal magmatism north of the Denali Fault system with Jumbo Dome (Cameron et al., 2015) and Buzzard Maar (Andronikov & Mukasa, 2010) being historical volcanos ~575 km from the modern trench (Figures 19.1 and 19.7). Similar to the Western Alaska Range Arc, periods of peak magmatism are ca. 95 Ma, ca. 60 Ma, and ca. 40 Ma (Figure 19.4). There are no substantial east–west or north–south trends with time except a gap in magmatism from ~87 to ~75 Ma when it shifted outboard to the Talkeetna Mountains and the southern Western Alaska Range (Figure 19.3).

19.4.3. Talkeetna Mountains

We compiled 86 bedrock ages and 2817 single-grain U-Pb zircon ages from the Talkeetna Mountains (Figures 19.3–19.6; references in supporting information S3). The Talkeetna Mountains have periods of peak magmatism of ca. 80 Ma, ca. 58 Ma, and ca. 45 Ma (Figure 19.4) (e.g., Finzel, 2019; Terhune et al., 2019). This area is mostly south of the *ARSZ,* but is shown for completeness. The ca. 80 Ma magmatic peak occurs during a period when magmatism ceases in the Central Alaska Range Arc (ca. 87 to 75 Ma) (Figure 19.3). The ca. 58 Ma and ca. 45 Ma magmatic peaks in the Talkeetna

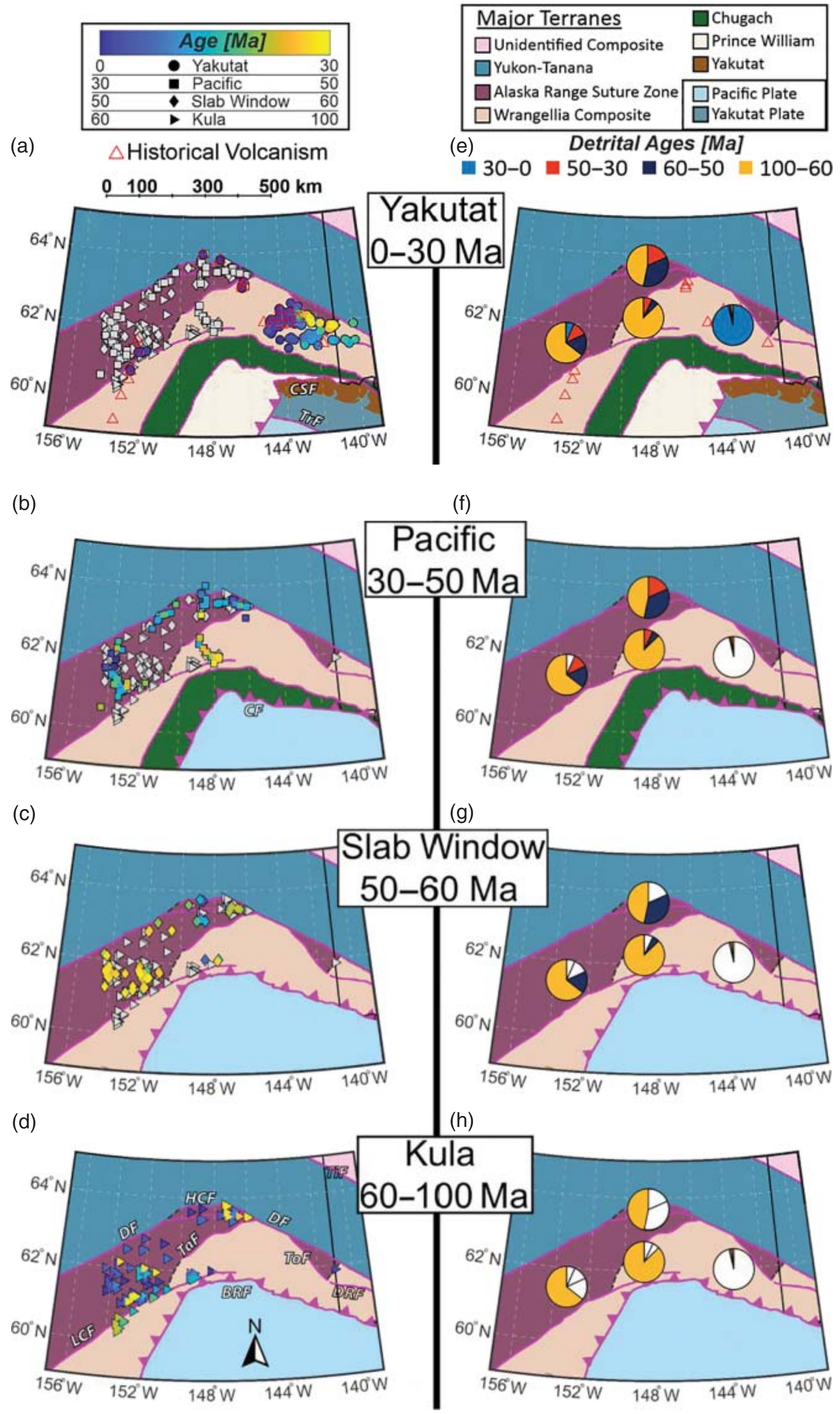

Figure 19.5 Compilations of magmatic ages in four main time periods. Map backgrounds are major regional terranes. The trench is moved to the position of each time period's outboard terrane. Within each time period, data points are plotted with color representing age, at the sampled location. Samples with ages from previous periods are in gray. (a–d) Bedrock ages. (e–h) Detrital ages. (a,e) Modern Yakutat slab dominated configuration (30–0 Ma). (b,f) Pacific dominated subduction configuration (50–30 Ma). (c,g) Slab window configuration, after Kula Plate breakoff (60–50 Ma). (d,h) Kula subduction configuration (100–60 Ma). TiF, Tintina Fault; DF, Denali Fault; HCF, Hines Creek Fault; TaF, Talkeetna Fault; LCF, Lake Clark Fault; ToF, Totschunda Fault; DRF, Duke River Fault; BRF, Border Ranges Fault; CF, Contact Fault; CSF, Chugach-St. Elias Fault; TrF, Transition Fault. Data are available in supporting information Tables S1–S4 on the companion website. For the Western and Central Alaska Range arcs, the 50–30 Ma division is data from 50 to 25 Ma because magmatism continues for 5 Ma after the arrival of the Yakutat slab.

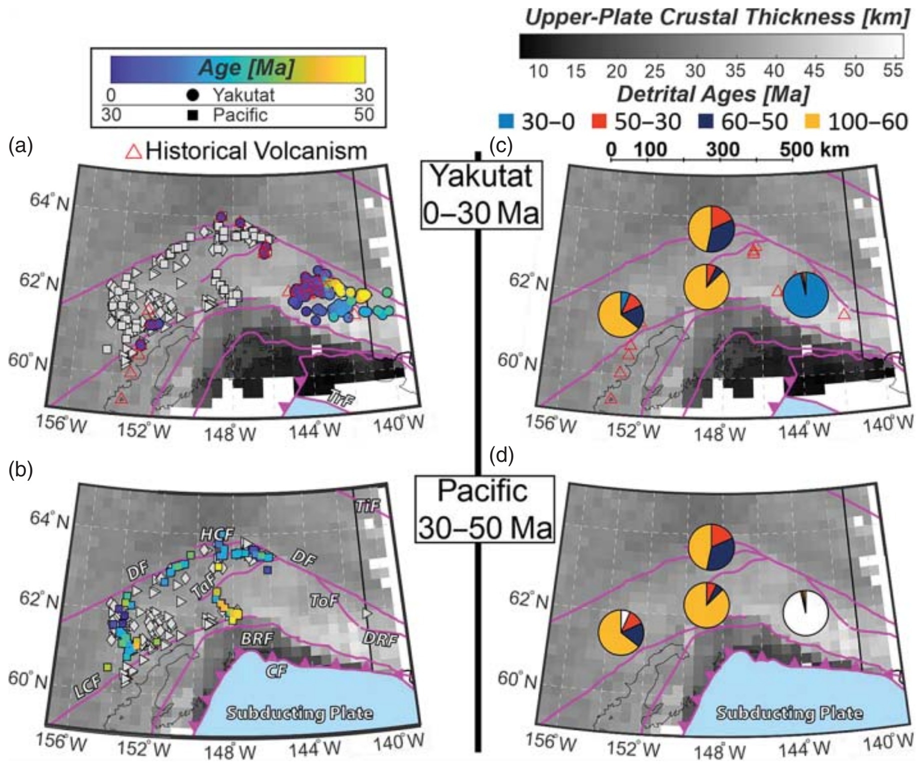

Figure 19.6 Compilations of ages in four main time periods. The map background is crustal thickness average from the synthesis work published in this monograph (Yang et al., 2024). (a,b) Bedrock ages. (c,d) Detrital ages. (a,c) Modern configuration (30–0 Ma). (b,d) Pacific subduction configuration (50–30 Ma). Kula subduction configuration (100–60 Ma) and slab window configuration (60–50 Ma) are not shown due to unknowns about paleocrustal thickness. All labels as in Figure 19.5.

Mountains reflect the slab window and relict slab window magmatism (Cole et al., 2006, 2007).

19.4.4. Wrangell Arc

We compiled 246 bedrock ages and 4,347 single-grain ages (U-Pb zircon and $^{40}Ar/^{39}Ar$ lithic grain ages) from the Wrangell Arc region (Figures 19.3–19.6; references in supporting information S4). The swath of Wrangell Arc magmatism along the *ARSZ* proceeds from ca. 100 Ma to Recent based on the compilation of both bedrock and detrital geochronology data sets (Berkelhammer et al., 2019; Brueseke et al., 2019; Richter et al., 1990; Trop et al., 2022). The detrital data set is more diverse than the bedrock data set, which likely reflects preferential bedrock sampling of Wrangell-aged lavas (<30 Ma; Brueseke et al., 2019) and glacier cover access concerns. Wrangell Arc periods of peak magmatism are ca. 60 Ma and ca. 30 Ma to Recent (Figure 19.4). Wrangell Arc magmatism occurs south of the Denali Fault for the entirety of its existence, but shifts slightly with time generally from the north (ca. 30 to 18 Ma) to the east (ca. 18 to 13 Ma), to the west (ca. 13 to 16 Ma), and finally to a distinct northwest progressing trend of 6 to 1 Ma (see Trop et al., 2022). From 30 to 6 Ma, magmatism is also focused along the Totschunda and Duke River faults with limited magmatism along the Totschunda Fault, 6 Ma to Recent (Trop et al., 2022).

19.4.5. Compiled Alaska Suture Zone Magmatic History

The combined data sets show peak periods of magmatism along the *ARSZ* at ca. 95 Ma, ca. 60 Ma, ca. 40 Ma, and Recent (Figure 19.4). The Wrangell Arc area has a slightly different history, reflecting the shutting off of the Western and Eastern Alaska Range arcs at ca. 25 Ma (Benowitz et al., 2022a; Jones III et al., 2021; Trop et al., 2019) and the initiation of the Yakutat slab related Wrangell Arc at ca. 30 Ma (Trop et al., 2022).

19.4.6. Geophysics Compilation

The overriding plate crust has a northward-thickening wedge shape from roughly 10 to 40 km thick under the Chugach-Prince William terrane and is at 35–55 km

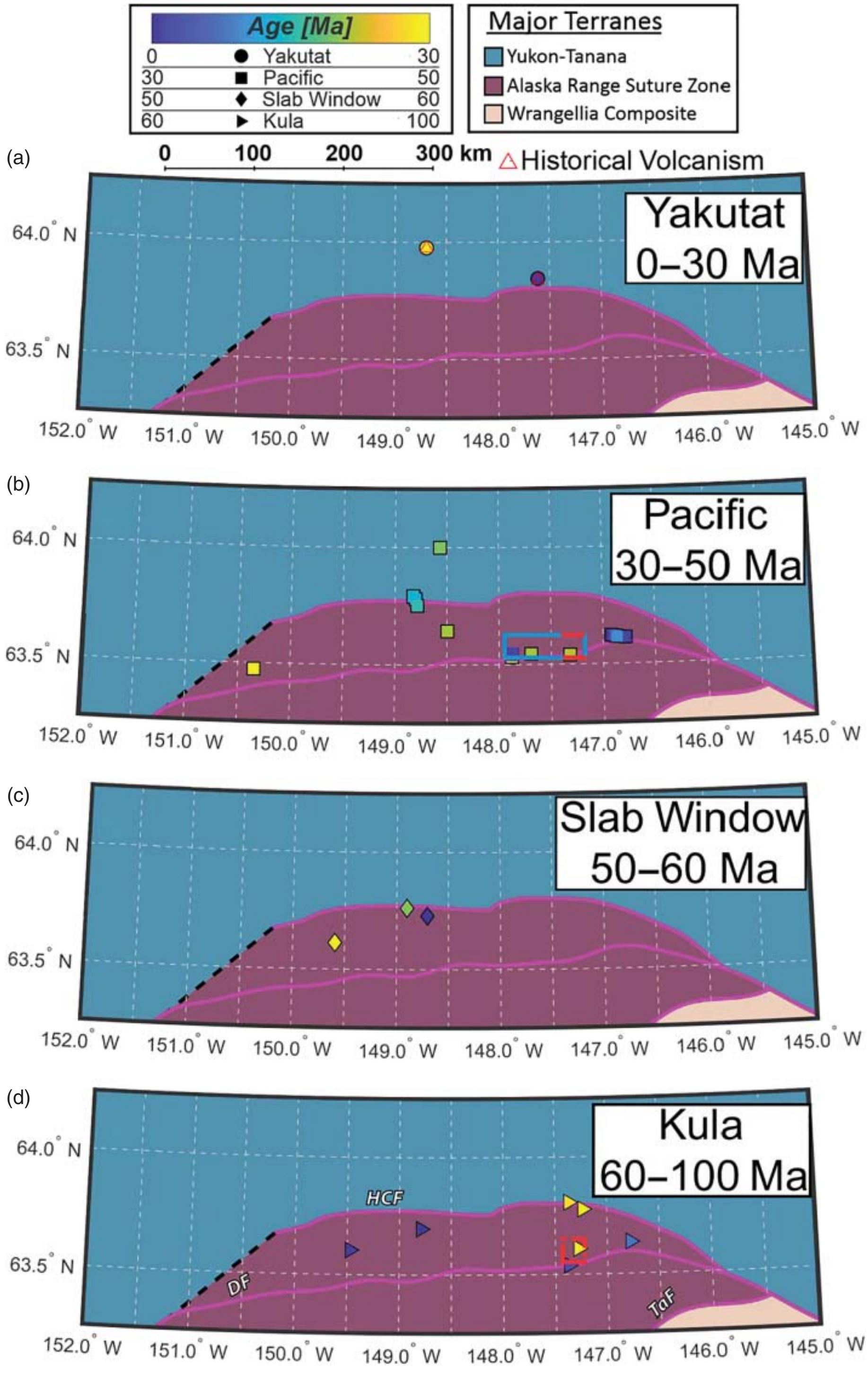

Figure 19.7 Compilations of ages in four main time periods for the apex of the ARSZ and north of the Denali Fault. Map backgrounds are major regional terranes. (a–d) Bedrock ages. (a) Modern configuration (30–0 Ma). (b) Pacific subduction configuration (50–30 Ma). (c) Slab window configuration (60–50 Ma). (d) Kula subduction configuration (100–60 Ma). Red box: ~97, ~63, and ~39 Ma plutons. Blue box: ~97, ~63, and ~39 Ma plutons and ~25 Ma mafic dikes. All labels as in Figure 19.5.

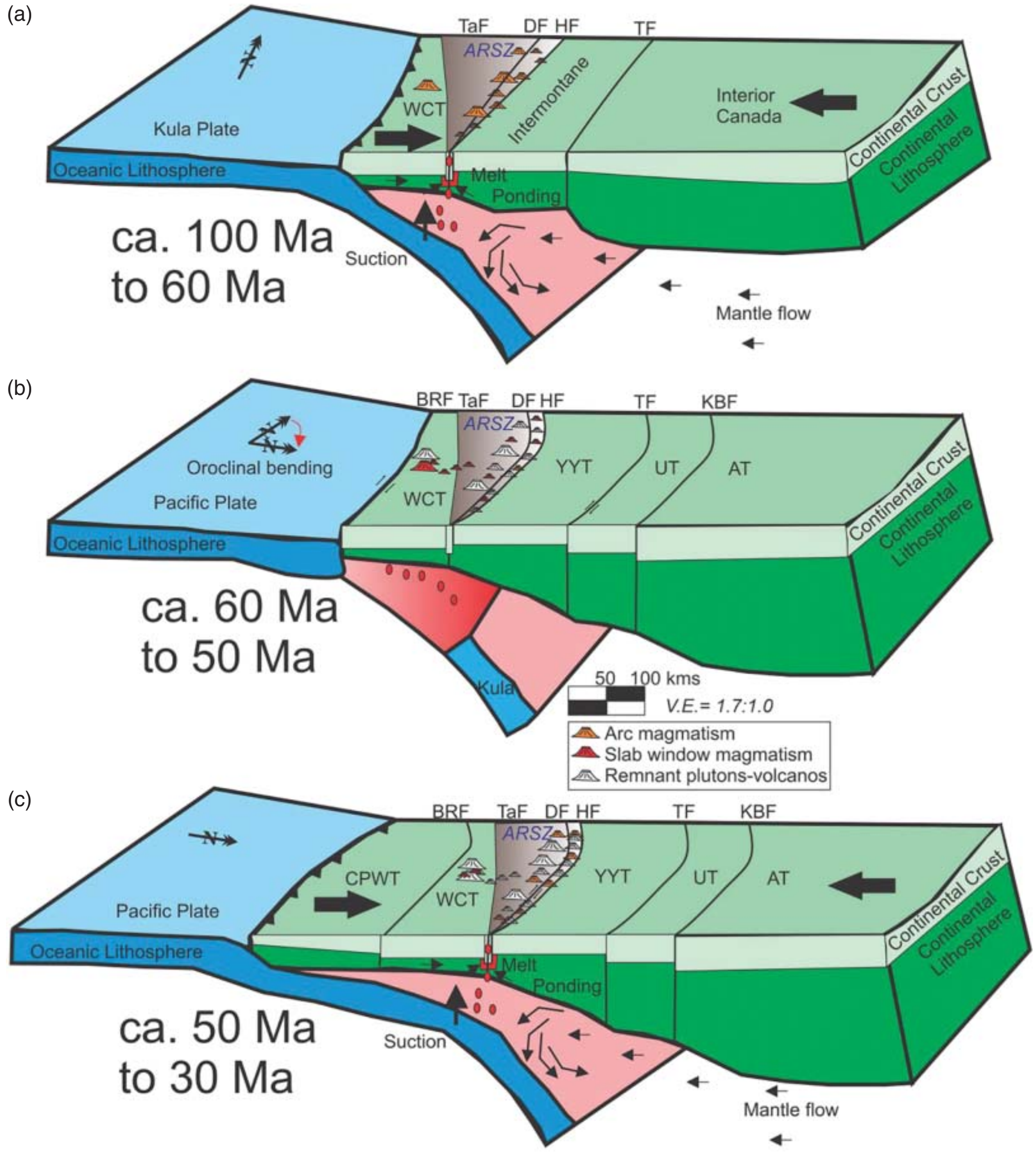

Figure 19.8 Schematics of four distinct periods of Central Alaska Range Arc magmatism. (a) After the mid-Cretaceous docking of the Wrangellia composite terrane off the coast of the Western USA/Western Canada (e.g., Tikoff et al., 2023; Trop et al., 2020), there was a long period of "normal" subduction from ca. 100 to 60 Ma with arc magmatism focused in the *ARSZ* with minor magmatism north of the Border Ranges Fault (Bleick et al., 2012). (b) The Alaska convergent margin was likely a transform system from ca. 60 to 50 Ma after break off of the Kula slab (Terhune et al., 2019). During this time period, 44° ± 11° counterclockwise oroclinal bending was occurring (Coe et al., 1989) and slab window magmatism in the *ARSZ* and to the south along the hinge of the orocline (Cole et al., 2006). (c) After accretion of the Chugach-Prince William Terrane (Garver & Davidson, 2015) and a Pacific Plate motion change at ca. 50 Ma (Sharp & Clague, 2006), subduction reinitiated and the trench jumped outboard about ~200 km. There was minor postslab window magmatism north of the Border Ranges Fault (e.g., Terhune et al., 2019) with magmatism once again focused in the *ARSZ*. (d) At ca. 30 Ma, the Yakutat oceanic plateau started to subduct under Alaska (Brueseke et al., 2019). Recent surmised mantle flow and calculated surface velocity directions from McConeghy et al. (2022) are inferred to be similar during past subduction regimes. North arrow rotates with paleolocation of the Wrangell composite terrane (e.g., Tikoff et al., 2023). AT, Arctic Plate; UT, Unidentified Terranes; YTT, Yukon Tanana Terrane; ARSZ, Alaska Range suture zone; WCT, Wrangellia composite terrane; CPWT, Chugach-Prince William Terrane; KF, Kobuk Fault; TF, Tintina Fault; HF, Hines Creek Fault; DF, Denali Fault; TaF, Talkeetna Fault; BRF, Border Ranges Fault. Scale bar is approximate.

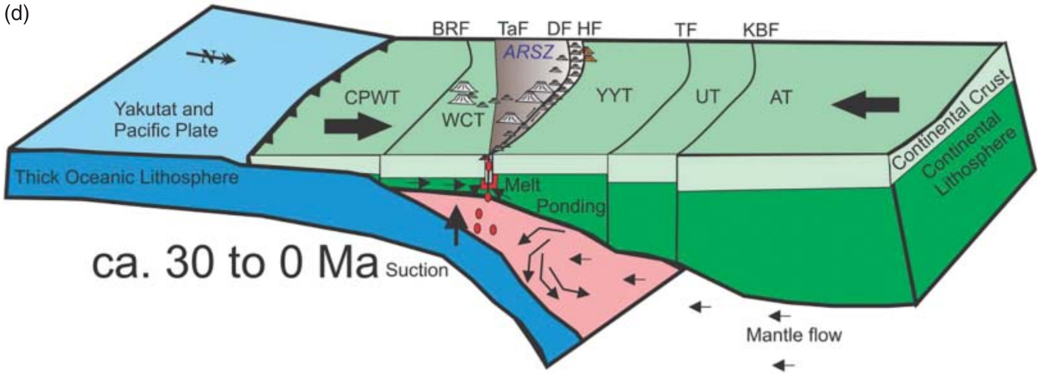

Figure 19.8 (*continued*)

under the Wrangellia composite terrane, 35–40 km under the *ARSZ*, 25 km under the Yukon Tanana Terrane, 35–40 km thick north of the Tintina Fault, and almost 50 km thick north of the Kobuk Fault under the Arctic Plate (Figures 19.2, 19.6, and 19.8) (Brennan et al., 2011; Gama et al., 2022; Mann et al., 2022; Miller et al., 2018; Rossi et al., 2006; Veenstra et al., 2006; Yang et al., 2024). There are Moho offsets across each of these tectono-boundaries. The upper-plate lithosphere thickness of the Chugach-Prince William Terrane is difficult to discern in places because of the underplating of the Yakutat slab and possible removal during Yakutat flat slab subduction, but extends to ~50 km depth in places (Fuis et al., 2008; Gama et al., 2022). The upper-plate lithosphere extends to ~50 km depth beneath the Wrangellia composite terrane, and the *ARSZ* is 65–125 km thick beneath the Yukon Tanana Terrane, 125–145 km thick beneath the region the north of the Tintina Fault, and up to 200 km thick north of the Kobuk Fault under the Arctic Plate (Figures 19.2 and 19.8) (Gama et al., 2022; Jiang et al., 2018; Miller et al., 2018; O'Driscoll & Miller, 2015).

The Western Alaska Range Arc generally follows the *ARSZ*, which has an east–west crustal thickness step (Figures 19.2 and 19.7) (Gama et al., 2022) and a strong magnetic signature gradient (Saltus & Hudson, 2022). The Central Alaska Range Arc is located primarily south of the Hines Creek Fault and borders both sides of the Denali Fault system in the *ARSZ* (Figures 19.5 and 19.7). There is a crustal thickness step across both the Denali (Allam et al., 2017) and Hines Creek faults (Allam et al., 2017; Brennan et al., 2011) (Figure 19.6), and a strong magnetic signature break across the Talkeetna Fault (Saltus & Hudson, 2022). The Wrangell Arc is located in the *ARSZ* where there is also a crustal thickness step (Figure 19.6) (Allam et al., 2017) and a magnetic signature break (Saltus & Hudson, 2022).

19.5. DISCUSSION

19.5.1. Arc Localization in the Alaska Range Suture Zone Since ca. 100 Ma

The Central Alaska Range Arc is dissected by the Cretaceous Denali Fault and the Western Alaska Range Arc is displaced to the west (Figure 19.1) (Benowitz et al., 2014; Miller et al., 2002). Known Cenozoic displacement amounts vary from east to west along the Denali Fault with ~480 km of displacement since ca. 52 Ma to the east and ~155 km of displacement since ca. 37 Ma to the west. As the ARSZ was translated to the west along the Denali Fault, the Central and Western Alaska Range arcs continued to be emplaced in the same mobile crustal block it had been emplaced before ca. 52 Ma. The ARSZ has been displaced ~180 km between ca. 30 Ma and 6 Ma along the Denali Fault (Trop et al., 2022), and ~125 km along the Totschunda Fault (Rosenthal et al., 2024) where the Yakutat slab related Wrangell Arc was emplaced (Brueseke et al., 2019). The modern ca. 30 Ma to Recent Wrangell Arc continued to be placed in the same mobile block, as the ARSZ was translated inboard and west along the Denali and Totschunda faults (Figure 19.1) (Trop et al., 2022).

The apex region of the ARSZ is located between the Hines Creek Fault and the Denali Fault and has not been translated along the Denali Fault. Figure 19.7 demonstrates that this region, located furthest inboard, in itself demonstrates arc localization since ca. 100 Ma. For example, an ~10 km long (south–north) × ~5 km across (east–west) swath has an ~97 Ma pluton intruded by an ~63 Ma pluton that was subsequently intruded by an ~39 Ma pluton (red box in Figure 19.7). Increasing the same swath 20 km to the east captures other ~60 Ma and ~39 Ma intrusions and ~25 Ma mafic dikes intruding the

~40 Ma plutons (blue box on Figure 19.7). If the same swath is increased to ~50 km (south-north) then recent ~10,000 ka magmatism is captured (Buzzard Maar; Figures 19.1 and 19.7).

Overall, based on the mapped compilation (N = 6,485 ages total) of detrital single grain and bedrock sample ages, continental arc magmatism has been localized along the *ARSZ* since ca. 100 Ma (Figures 19.1, 19.3–19.7). This arc localization (1) occurred as far as ~300 and 575 km from a subduction trench that generally moved oceanward with time through accretion (Garver & Davidson, 2015; Trop et al., 2019), (2) occurred in segments of the upper plate that were mobile along regional lithospheric and crustal-scale strike-slip faults (Gama et al., 2022; Waldien et al., 2021), (3) involved slabs of different ages (Engebretson et al., 1984; Wells et al., 2014), variable convergence angles and velocities (Doubrovine & Tarduno, 2008; Jicha et al., 2018; Sharp & Clague, 2006), and varying thicknesses (Mann et al., 2022; Worthington et al., 2012), (4) was maintained after oroclinal bending that greatly modified the margin geometry (e.g., Gillis et al., 2022) and slab break off resulting in a slab window event (Terhune et al., 2019), and (5) mostly occurred south of the Denali Fault system (including the Hines Creek segment) along the *ARSZ* from ca. 100 Ma to Recent.

By deduction, preexisting features of the Alaska upper plate must be playing a first-order role in localizing magmatism. Sutures can act as passive conduits for magma (Richards, 2003) and play an active role in magmatism localization (Gómez-Vasconcelos et al., 2020). However, melt generally rises vertically (Hall & Kincaid, 2001) and slabs subducting under the *ARSZ* must have maintained a depth of around 130 ± 70 km (England et al., 2004; van Keken et al., 2011; Isacks & Barazangi, 1977; Syracuse & Abers, 2006) since 100 Ma to generate melt in the general vicinity of the *ARSZ*. Furthermore, there is no dominant structure along the spine of the Western Alaska Range Arc to facilitate arc magmatism localization (Figure 19.1), implying arc localization controls beyond lithospheric scale structural conduits.

19.5.2. Mechanisms for Arc Localization in the *ARSZ* Since ca. 100 Ma

The overriding plate in a subduction zone influences the geometry of the subducting slab through its effect on the mantle flow field: flow around the subducting slab can cause both low dynamic pressures above the slab and high dynamic pressures below the slab, and lead to forces that counteract negative slab buoyancy and decrease subducting dip angle (Liu, 2022; Rodríguez-González et al., 2012; Stevenson & Turner, 1977; Tovish et al., 1978). It has also been demonstrated through geodynamic modeling and natural examples that the presence of a region of thicker colder upper plate moving toward the trench can lead to increased mantle-flow-related hydrodynamic "suction" in the mantle wedge (van Hunen et al., 2004; Manea & Gurnis, 2007; Rodríguez-González et al., 2012, 2014). Thus, slab dips beneath continents are generally shallower by ~20° than under oceanic lithosphere and flat slab subduction under oceanic lithosphere has not been documented (England et al., 2004; Jarrard, 1986; Syracuse & Abers, 2006).

Based on paleomagnetic reconstructions, at ca. 80 Ma the Wrangellia composite terrane of Alaska was at a paleolatitude of 53° ± 8°N (Stamatakos et al., 2001) and by ca. 50 Ma this terrane was at or near modern latitudes (Panuska et al., 1990). More speculatively, at ca. 100 Ma the Wrangellia composite terrane of Alaska may have been located off the coast of the western United States (e.g., Tikoff et al., 2023). The incoming slab (Doubrovine & Tarduno, 2008; Madsen et al., 2006, e.g., Pavlis et al., 2019) as well as the inboard upper-plate thickness and thermal characteristics varied (e.g., Estève et al., 2020; Gama et al., 2022; Yuan & Romanowicz, 2010) along the >2,000 km northward translation of the Wrangellia composite terrane. Regardless of the exact paleolatitude position, the Wrangellia composite terrane would have been outboard of a plate with a thicker (>100 km) lithosphere (Porter & Reid, 2021) when translated north along the modern-day western United States (Figure 19.8a). At ca. 80, when the Wrangellia composite terrane was being translated along the coast of modern-day British Columbia, the inboard lithosphere would have been relatively thin (~80–100 km thick) (Clowes et al., 1995). Interestingly, this is the time when arc magmatism ceased in the Central Alaska Range and shifted outboard to the Western Alaska Range and Talkeetna Mountains, which suggests slab steepening or rollback during this time period or possibly the translation of the Wrangellia composite terrane over a steeper dipping slab segment. The trench distance to the thick-cold craton for the Wrangellia composite terrane would have been ~350 km from the >150 km thick Mackenzie craton when passing by the modern-day Yukon Territory around ca. 75 Ma when arc magmatism re-initiated in the Central Alaska Range (Estève, 2020; Estève et al., 2020; Schaeffer & Lebedev, 2014). If subduction processes and associated mantle flow under a mobile Wrangellia composite terrane led to lithospheric removal of inboard cratons (Cooper et al., 2021) or if these cratons underwent slab under-platting (Taramón et al., 2015) is an open question.

The period of ca. 60 to 50 Ma was a dynamic period in Alaska history with the Kula Plate breaking off, the creation of a slab window under southern Alaska, the final translation of the Chugach-Prince William Terrane into place, and syn-tectonic oroclinal bending (Figure 19.8b) (Garver & Davidson, 2015; Gillis et al., 2022; Terhune et al., 2019). The shape of the trench was modified at this time, as was any preexisting subduction channel-slab-related mantle features. However, when subduction reinitiated at ca. 48 Ma (Benowitz et al., 2022a; Bezard et al., 2021; Jones III et al., 2021), the continental arc once again returned to the *ARSZ*.

The lithosphere north of the Denali Fault system is of Laurentian (Dusel-Bacon et al., 2013, 2017; Jones et al., 2017) and Caledonian affinity (McClelland et al., 2021), whereas the terranes of southern Alaska are primarily of oceanic affinity (e.g., Trop & Ridgway, 2007). This contrast is clear in both the lithosphere being thicker and colder north and west of the *ARSZ* (Gama et al., 2022). Additionally, the lithosphere beneath northern Alaska is even thicker (150–200 km) and colder (Figure 19.8c) (Gama et al., 2022; Jiang et al., 2018; O'Driscoll & Miller, 2015). Alaska/North America has been moving to the southwest since the late Cretaceous (e.g., Tikoff et al., 2023) leading to an overall trenchward motion of interior Alaska that continues today (McConeghy et al., 2022). Hence, we prefer a geodynamic model where the upper-plate lithospheric shape and dynamics induce hydrodynamic "suction" forces that have controlled the geometry of the underlying Alaska slab since ca. 100 Ma. The ca. 30 Ma to Recent flat/shallow slab subduction of the Yakutat oceanic plateau beneath Alaska also likely reflects a component of upper-plate hydrodynamic "suction" (Figure 19.8d). Many studies have demonstrated that anomalously thick/buoyant oceanic slabs alone do not lead to shallow subduction, but also need a component of mantle-wedge suction (O'Driscoll et al., 2009; Manea et al., 2012; Skinner & Clayton, 2013).

Additional features of the upper plate are also likely contributing to arc localization in the *ARSZ*. Suture zones, which are regions of crustal weakness (Sykes, 1978), can act as pathways that funnel rising melt (Dahm et al., 2020). It has also been suggested that upper-plate faults that penetrate all the way through the crust (e.g., Vauchez et al., 2012) can funnel slab-related melts into the upper crust (Marot et al., 2014), and it has been documented that extensional kinematic environments along strike-slip faults can lead to magmatism localization (Gómez-Vasconcelos et al., 2020; Mathieu et al., 2011; Tibaldi et al., 2017; Webb et al., 2020). The Hines Creek, Denali, and Totschunda faults bounding the northern *ARSZ* are Cretaceous and still active (Benowitz et al., 2014, 2022a, 2022b; Miller et al., 2002; Trop et al., 2020), lithospheric-scale (Allam et al., 2017; Eberhart-Phillips et al., 2003; Gama et al., 2022) strike-slip faults (Figure 19.8). Eocene-dissected plutons (Regan et al., 2021), fault zone extension related Cretaceous–Oligocene–Miocene dike swarms (Brueseke et al., 2019; Trop et al., 2019, 2020), and Cretaceous-to-Recent magmatism focused along the Denali and Totschunda faults (Waldien et al., 2021; Benowitz et al., 2022a; Trop et al., 2012, 2022; Gillis et al., 2022) support these structures having an active role in arc magmatism localization.

Another scenario leading to arc localization along the *ARSZ* since ca. 100 Ma is possible melt ponding along Totschunda and Denali fault Moho depth offsets (Figures 19.2 and 19.8). Melt ponding has been inferred below upper-plate structures from seismic imaging (e.g., MacKenzie et al., 2008; Rondenay et al., 2010). We speculate that inherited Cretaceous Moho depth offsets, such as those across the Totschunda and Denali fault systems (e.g., Allam et al., 2017; Gama et al., 2022), may be acting as catchments for melt rising through the convecting mantle wedge and hence contribute to focusing magmatism along crustal-scale structures.

19.5.3. Potential Avenues for Future Alaska Range Suture Zone Magmatism Research

Further interdisciplinary work can buttress and test our interpretations of 100 million years of localized *ARSZ* arc magmatism due to upper-plate-controlled hydrodynamic mantle wedge suction forces. A lack of geochemical constraints on many of the bedrock samples compiled for this work (e.g., Trop et al., 2019; e.g., Jones III et al., 2021) raises the question if all periods of *ARSZ* "arc" magmatism described here have been related to underlying slab processes. In particular, it is possible that the ∼100–90 Ma dated plutons of the *ARSZ* might be related to the diachronous suturing of Wrangellia with the Yukon Tanana Terrane and hence collisional magmatism. It is also possible that arc magmatism has been localized along the *ARSZ* before ∼100 Ma, as suggested by the ∼117 to ∼100 (?) Ma continental Chisana Arc (Manselle et al., 2020; Rosenthal et al., 2024; Trop et al., 2020). If there is a long history (∼100 Ma to Recent) of toroidal flow and associated slab edge upwelling magmatism along regions of Wrangellia, as has been proposed for parts of the Wrangell Arc (Jadamec & Billen, 2010, 2012), and if this process played a possible role in arc magmatism localization, then it deserves expanded geochemical and computational modeling investigations.

The paleolatitude constraints and translation history of Wrangellia could be improved (e.g., Tikoff et al., 2023), which would allow better matching of periods of localized *ARSZ* magmatism and inboard lithospheric thickness variations along western North America. There is also potential to use plutons from the *ARSZ* as tie-in points to assist with reconstructions of the northward translation of Wrangellia along North America's western margin.

We further propose that computational modeling (e.g., Manea et al., 2012) could possibly test the hypotheses presented here and in particular determine to what extent the Yakutat slab shallow dipping geometry is affected by upper-plate thickness heterogeneity, mantle dynamics, and mantle wedge hydrodynamic processes. How ~100 million years of thermal weakening and mantle upwelling affects fault localization (Benowitz et al., 2022a, 2022b; e.g., Liu & Currie, 2022) and topographic development along the Denali Fault (Benowitz et al., 2019; Jadamec et al., 2013) also warrants further study.

19.5.4. Other Examples of Long-Lived Arc Localization

Globally, there are many past and present examples of localized arc magmatism. The Gangdese arc of southern Tibet was broadly localized ca. 100–45 Ma (Ma et al., 2022). Magmatism has been returning to a suture zone region of northwest Iran with late Carboniferous, mid-Cretaceous, and middle Eocene magmatic events (Zhang et al., 2023) and Eocene to late Miocene localized magmatism (Rabiee et al., 2020). Magmatism was localized along the Burma Plate during Cretaceous and Eo-Oligocene arc magmatic events while the plate was being translated >2,000 km and undergoing different subduction orientations/slab configurations (Licht et al., 2020; Westerweel et al., 2019).

The Cascade Arc has been emplaced along the same general region of crust since ca. 45 Ma (Humphreys & Grunder, 2022), with Eocene, Oligocene, Miocene, Pliocene, and Pleistocene magmatic products intruded next to and through one another. Even classic examples of long-lived arcs such as the northern Andes (Ducea et al., 2015) appear to be emplaced along preexisting suture zones. About 70 million years of arc magmatism in South America has generally been emplaced along the Peletec suture zone in Ecuador with no Cenozoic arc magmatic products emplaced to the east into the South American craton (Chiaradia et al., 2004; Glazner, 2022). Furthermore, Farrar et al. (2023) documented Paleocene to Miocene arc magmatism localized along vertical lithospheric faults.

Our results in Alaska suggest that these and other regions of long-lived arc localization reflect the geodynamic influence of upper-plate hydrodynamic "suction" on underlying slab geometry (O'Driscoll et al., 2009). Additionally, inherited lithospheric thickness heterogeneity along suture zones provides a fundamental environment for potential long-lived localized arc magmatism.

19.6. CONCLUSION

We document ca. 100 million years of continental magmatic arc spatial localization along the *ARSZ* of the mobile southern Alaska Wrangellia composite terrane by compiling 6,485 total bedrock and single grain detrital ages in the framework of a trench that moves outboard through successive accretion events (Figures 19.5 and 19.8). For example, repeated periods of arc magmatism in the Central Alaska Range Arc, located at times >500 km from the trench, highlight a first-order upper-plate control on magmatic spatial patterns. By deduction, inherited features of the upper plate must be controlling both the geometry (e.g., dip) of the underlying slab and potentially focusing melt transport. Arc localization since ca. 100 Ma has been in part controlled by inferred upper-plate-related hydrodynamic (viscous) mantle wedge "suction" forces driven by trenchward motion of thick-cold lithosphere (>100 km and up to 200 km thick in places) inboard of the Wrangellia composite terrane (Figures 19.2 and 19.8).

While the geoscience community has justifiably been focused on trench-perpendicular magmatic arc migration (e.g., Gianni & Luján, 2021) due to the dynamic nature of convergent margins and the important processes related to slab rollback and advance that arc migrations reflect, magmatic arc localization may be an underappreciated geodynamic process with implications for first-order upper-plate control on slab geometry and magma ascent processes. Hence, we recommend time-dependent numerical modeling to further evaluate the influence of these hydrodynamic "suction" forces on the shallow subduction geometry of the Yakutat oceanic plateau. Additionally, matching pulses and gaps in arc magmatism along North America's western margin with the magmatic record of the Wrangellia composite terrane may provide further buttressing for the established "Baja-Alaska" paradigm (e.g., Boivin et al., 2022; Tikoff et al., 2023).

ACKNOWLEDGMENTS

We would like to acknowledge Chris Nye for inspiring this work with a dissertation defense question and we thank Jeff Trop and Matt Brueseke for helpful discussions on the subject of southern Alaska's magmatic history. This work was partially funded by NSF EAR-2053042 and Woods Hole Oceanographic Institution OBS Instrument Center Postdoctoral Scholarship to Michael Everett Mann. We appreciate the helpful, detailed, and constructive suggestions of three anonymous reviewers and volume editor Margarete Jadamec.

AVAILABILITY STATEMENT

The data are available in the supporting information files and can also be accessed in the Zenodo Repository (https://zenodo.org/record/7592004#.Y9mhhK3MK3A).

REFERENCES

Allam, A. A., Schulte-Pelkum, V., Ben-Zion, Y., Tape, C., Ruppert, N., & Ross, Z. E. (2017). Ten kilometer vertical Moho offset and shallow velocity contrast along the Denali fault zone from double-difference tomography, receiver functions, and fault zone head waves. *Tectonophysics*, *721*, 56–69. https://doi.org/10.1016/j.tecto.2017.09.003

Alvarado, A., Audin, L., Nocquet, J. M., Jaillard, E., Mothes, P., Jarrín, P., et al. (2016). Partitioning of oblique convergence in the Northern Andes subduction zone: Migration history and the present-day boundary of the North Andean Sliver in Ecuador. *Tectonics*, *35*(5), 1048–1065.

Anders, M. H. (1994). Constraints on North American plate velocity from the Yellowstone hotspot deformation field. *Nature*, *369*(6475), 53–55.

Andronikov, A. V., & Mukasa, S. B. (2010). $^{40}Ar/^{39}Ar$ eruption ages and geochemical characteristics of Late Tertiary to Quaternary intraplate and arc-related lavas in interior Alaska. *Lithos*, *115*(1–4), 1–14.

Arce, J. L., Ferrari, L., Morales-Casique, E., Vasquez-Serrano, A., Arroyo, S. M., Layer, P. W., et al. (2020). Early Miocene arc volcanism in the Mexico City Basin: Inception of the Trans-Mexican volcanic belt. *Journal of Volcanology and Geothermal Research*, *408*, 107104.

Athey, J. E., Newberry, R. J., Werdon, M. B., Freeman, L. K., Smith, R. L., & Szumigala, D. J., (2006). Bedrock geologic map of the Liberty Bell area, Fairbanks A-4 Quadrangle, Bonnifield mining district, Alaska. *Alaska Division of Geological & Geophysical Surveys Report of Investigation 2006-2*, 1.0.1, scale 1:50,000, 1 sheet, 98 p. text. doi:10.14509/15026.

Austermann, J., Ben-Avraham, Z., Bird, P., Heidbach, O., Schubert, G., & Stock, J. M. (2011). Quantifying the forces needed for the rapid change of Pacific plate motion at 6 Ma. *Earth and Planetary Science Letters*, *307*(3–4), 289–297.

Benowitz, J. A., Cooke, M. L., Terhune, P. J., Herreid, S., Bemis, S. P., Toeneboehn, K., et al. (2022b). Why is Denali (6,194 m) so big? Caught inside the tectonic wake of a migrating restraining bend. *Terra Nova*, *34*(2), 123–136.

Benowitz, J. A., Haeussler, P. J., Layer, P. W., O'Sullivan, P. B., Wallace, W. K., & Gillis, R. J. (2012). Cenozoic tectono-thermal history of the Tordrillo Mountains, Alaska: Paleocene-Eocene ridge subduction, decreasing relief, and late Neogene faulting. *Geochemistry, Geophysics, Geosystems*, *13*(4).

Benowitz, J. A., Layer, P. W., & Vanlaningham, S. (2014). Persistent long-term (c. 24 Ma) exhumation in the Eastern Alaska Range constrained by stacked thermochronology. *Geological Society, London, Special Publications*, *378*(1), 225–243.

Benowitz, J. A., Davis, K., & Roeske, S. (2019). A river runs through it both ways across time: $^{40}Ar/^{39}Ar$ detrital and bedrock muscovite geochronology constraints on the Neogene paleodrainage history of the Nenana River system, Alaska Range. *Geosphere*, *15*(3), 682–701.

Benowitz, J. A., Roeske, S. M., Regan, S. P., Waldien, T. S., Elliott, J. L., & O'Sullivan, P. B. (2022a). Large-scale, crustal-block vertical extrusion between the Hines Creek and Denali faults coeval with slip localization on the Denali fault since ca. 45 Ma, Hayes Range, Alaska, USA. *Geosphere*, *18*(3), 1030–1054.

Berkelhammer, S. E., Brueseke, M. E., Benowitz, J. A., Trop, J. M., Davis, K., Layer, P. W., & Weber, M. (2019). Geochemical and geochronological records of tectonic changes along a flat-slab arc-transform junction: Circa 30 Ma to ca. 19 Ma Sonya Creek volcanic field, Wrangell Arc, Alaska. *Geosphere*, *15*(5), 1508–1538.

Bezard, R., Hoernle, K., Pfänder, J. A., Jicha, B., Werner, R., Hauff, F., et al. (2021). $^{40}Ar/^{39}Ar$ ages and bulk-rock chemistry of the lower submarine units of the central and western Aleutian Arc. *Lithos*, *392*, 106147.

Billen, M. I., & Hirth, G. (2007). Rheologic controls on slab dynamics. *Geochemistry, Geophysics, Geosystems*, *8*(8).

Bleick, H. A., Till, A. B., Bradley, D. C., O'sullivan, P. B., Wooden, J. L., Bradley, D. B., et al. (2012). *Early Tertiary exhumation of the flank of a forearc basin, southwest Talkeetna Mountains, Alaska*. US Geological Survey Open-File Report, 1232-1.

Boivin, M. P., Matthews, W., Coutts, D., & Hubbard, S. (2022). Improved provenance constraints for Nanaimo Group sediments, British Columbia, Canada, through zircon LA-ICP-MS depth-profiling. *Tectonics*, e2021TC007106.

Box, S. E., Karl, S. M., Jones, J. V., III, Bradley, D. C., Haeussler, P. J., & O'Sullivan, P. B. (2019). Detrital zircon geochronology along a structural transect across the Kahiltna assemblage in the western Alaska Range: Implications for emplacement of the Alexander-Wrangellia-Peninsular terrane against North America. *Geosphere*, *15*(6), 1774–1808.

Brennan, P., Gilbert, H., & Ridgway, K. D. (2011). Crustal structure across the central Alaska Range: Anatomy of a Mesozoic collisional zone. *Geochemistry, Geophysics, Geosystems*, *12*(4).

Brueseke, M. E., Benowitz, J. A., Bearden, A. T., Mann, M. E., & Miggins, D. P. (2023b). Subduction disruption, slab tears: Ca. 1 Ma true collision of an ~30-km-thick oceanic plateau segment recorded by Yakutat slab nascent tear magmatism. *Terra Nova*, *35*, 1–9. https://doi.org/10.1111/ter.12628

Brueseke, M. E., Benowitz, J. A., Trop, J. M., Davis, K. N., Berkelhammer, S. E., Layer, P. W., & Morter, B. K. (2019). The Alaska Wrangell Arc:~ 30 Ma of subduction-related magmatism along a still active arc-transform junction. *Terra Nova*, *31*(1), 59–66.

Brueseke, M., Morter, B. K., Benowitz, J. A., Trop, J., Mertzman, S. A., Kirby, C. S., & Davis, K. (2023a). What lies beneath the ice? Using the geochemistry and geochronology of modern river cobbles to better decipher the evolution of a glaciated volcanic arc (Wrangell Arc, Alaska, USA). *Volcanica*, *6*(2), 313–329.

Cagnioncle, A. M., Parmentier, E. M., & Elkins-Tanton, L. T. (2007). Effect of solid flow above a subducting slab on water distribution and melting at convergent plate boundaries. *Journal of Geophysical Research: Solid Earth*, *112*(B9).

Cameron, C. E., (2005), Latitudes and longitudes of volcanoes in Alaska. *Alaska Division of Geological & Geophysical Surveys Raw Data File 2005-3*. https://doi.org/10.14509/7103.

Cameron, C. E., Crass, S. W., & AVO Staff. (Eds.) (2022). Geologic database of information on volcanoes in Alaska (GeoDIVA). In *Alaska Division of Geologic and Geophysical Surveys Digital Data Series 20*. https://doi.org/10.14509/30901

Cameron, C. E., Nye, C., Bull, K. F., & Woods, R. E. F. (2015). *Jumbo Dome, Interior Alaska: Whole-rock major-and trace-element analyses* (p. 3). State of Alaska, Department of Natural Resources, Division of Geological & Geophysical Surveys.

Chapman, J. B., & Ducea, M. N. (2019). The role of arc migration in Cordilleran orogenic cyclicity. *Geology*, *47*(7), 627–631.

Chiao, L. Y., Creager, K. C., Kirby, S., Wang, K., & Dunlop, S. (2002). Geometry and membrane deformation rate of the subducting Cascadia slab. *The Cascadia subduction zone and related subduction system—Seismic structure, intraslab earthquakes and processes, and earthquake hazards*, pp. 02–328.

Chiaradia, M., Fontboté, L., & Beate, B. (2004). Cenozoic continental arc magmatism and associated mineralization in Ecuador. *Mineralium Deposita*, *39*, 204–222.

Christeson, G. L., Gulick, S. P., van Avendonk, H. J., Worthington, L. L., Reece, R. S., & Pavlis, T. L. (2010). The Yakutat terrane: Dramatic change in crustal thickness across the Transition fault, Alaska. *Geology*, *38*(10), 895–898.

Clowes, R. M., Zelt, C. A., Amor, J. R., & Ellis, R. M. (1995). Lithospheric structure in the southern Canadian Cordillera from a network of seismic refraction lines. *Canadian Journal of Earth Sciences*, *32*(10), 1485–1513.

Coe, R. S., Globerman, B. R., & Thrupp, G. A. (1989). Rotation of central and southern Alaska in the early Tertiary: Oroclinal bending by megakinking? In C. Kissel & C. Laj (Eds.), *Paleomagnetic rotations and continental deformation* (pp. 327–342). Dordrecht: Springer.

Cole, R. B., Nelson, S. W., Layer, P. W., & Oswald, P. J. (2006). Eocene volcanism above a depleted mantle slab window in southern Alaska. *Geological Society of America Bulletin*, *118*(1–2), 140–158.

Cole, R. B., Layer, P. W., Hooks, B., Cyr, A., & Turner, J. (2007). Magmatism and deformation in a terrane suture zone south of the Denali fault, northern Talkeetna Mountains, Alaska. In K. D. Ridgway, J. M. Trop, J. M. G. Glen, & J. M. O'Neill (Eds.), *Tectonic growth of a collisional continental margin: Crustal evolution of southern Alaska* (pp. 55–94). Geological Society of America Special Paper 431. https://doi.org/10.1130/2007.2431(04)

Colpron, M., & Nelson, J. L. (2011). *A digital atlas of terranes for the northern Cordillera [Dataset]*. Accessed online from Yukon Geological Survey. Retrieved from www.geology.gov.yk.ca

Cooper, C. M., Farrington, R. J., & Miller, M. S. (2021). On the destructive tendencies of cratons. *Geology*, *49*(2), 195–200.

Dahm, T., Stiller, M., Mechie, J., Heimann, S., Hensch, M., Woith, H., et al. (2020). Seismological and geophysical signatures of the deep crustal magma systems of the Cenozoic volcanic fields beneath the Eifel, Germany. *Geochemistry, Geophysics, Geosystems*, *21*(9), e2020GC009062.

DeMets, C., & Dixon, T. H. (1999). New kinematic models for Pacific-North America motion from 3 Ma to present, I: Evidence for steady motion and biases in the NUVEL-1A model. *Geophysical Research Letters*, *26*(13), 1921–1924.

DeMets, C., Iaffaldano, G., & Merkouriev, S. (2015). High-resolution Neogene and quaternary estimates of Nubia-Eurasia-North America plate motion. *Geophysical Journal International*, *203*(1), 416–427.

Doubrovine, P. V., & Tarduno, J. A. (2008). A revised kinematic model for the relative motion between Pacific oceanic plates and North America since the Late Cretaceous. *Journal of Geophysical Research: Solid Earth*, *113*, 1–20.

Ducea, M. N., Saleeby, J. B., & Bergantz, G. (2015). The architecture, chemistry, and evolution of continental magmatic arcs. *Annual Review of Earth and Planetary Sciences*, *43*, 299–331.

Dusel-Bacon, C., Day, W. C., & Aleinikoff, J. N. (2013). Geochemistry, petrography, and zircon U–Pb geochronology of Paleozoic metaigneous rocks in the Mount Veta area of east-central Alaska: Implications for the evolution of the westernmost part of the Yukon–Tanana terrane. *Canadian Journal of Earth Sciences*, *50*(8), 826–846.

Dusel-Bacon, C., Holm-Denoma, C. S., Jones, J. V., Aleinikoff, J. N., & Mortensen, J. K. (2017). Detrital zircon geochronology of quartzose metasedimentary rocks from parautochthonous North America, east-central Alaska. *Lithosphere*, *9*(6), 927–952.

Eberhart-Phillips, D., Christensen, D. H., Brocher, T. M., Hansen, R., Ruppert, N. A., Haeussler, P. J., & Abers, G. A. (2006). Imaging the transition from Aleutian subduction to Yakutat collision in central Alaska, with local earthquakes and active source data. *Journal of Geophysical Research*, *111*.

Eberhart-Phillips, D., Haeussler, P. J., Freymueller, J. T., Frankel, A. D., Rubin, C. M., Craw, P., et al. (2003). The 2002 Denali fault earthquake, Alaska: A large magnitude, slip-partitioned event. *Science*, *300*(5622), 1113–1118.

Elliott, J. L., Larsen, C. F., Freymueller, J. T., & Motyka, R. J. (2010). Tectonic block motion and glacial isostatic adjustment in southeast Alaska and adjacent Canada constrained by GPS measurements. *Journal of Geophysical Research: Solid Earth*, *115*(B9).

Engebretson, D. C., Cox, A., & Gordon, R. G. (1984). Relative motions between oceanic plates of the Pacific basin. *Journal of Geophysical Research: Solid Earth*, *89*(B12), 10291–10310.

England, P., Engdahl, R., & Thatcher, W. (2004). Systematic variation in the depths of slabs beneath arc volcanoes. *Geophysical Journal International*, *156*(2), 377–408. https://doi.org/10.1111/j.1365-246X.2003.02132.x

Estève, C. (2020). *Evolution and tectonics of the lithosphere in Northwestern Canada*. Doctoral dissertation. Université d'Ottawa/University of Ottawa.

Estève, C., Audet, P., Schaeffer, A. J., Schutt, D. L., Aster, R. C., & Cubley, J. F. (2020). Seismic evidence for craton chiseling and displacement of lithospheric mantle by the Tintina fault in the northern Canadian Cordillera. *Geology*, *48*(11), 1120–1125.

Farrar, A. D., Cooke, D. R., Hronsky, J. M., Wood, D. G., Benavides, S. B., Cracknell, M. J., et al. (2023). A model for the lithospheric architecture of the central Andes and the localization of giant porphyry copper deposit clusters. *Economic Geology*, *118*(6), 1235–1259.

Fasulo, C. R., & Ridgway, K. D. (2021). Detrital zircon geochronology of modern river sediment in south-central Alaska: Provenance, magmatic, and tectonic insights into the Mesozoic and Cenozoic development of the southern Alaska convergent margin. *Geosphere*, *17*(4), 1248–1267.

Ferris, A., Abers, G. A., Christensen, D. H., & Veenstra, E. (2003). High resolution image of the subducted Pacific (?) plate beneath central Alaska, 50–150 km depth. *Earth and Planetary Science Letters*, *214*(3–4), 575–588.

Finzel, E. S. (2019). Partitioning pervasive detrital geochronologic age distributions in the southern Alaskan forearc. *Frontiers in Earth Science*, *7*, 217.

Fitzgerald, P. G., Roeske, S. M., Benowitz, J. A., Riccio, S. J., Perry, S. E., & Armstrong, P. A. (2014). Alternating asymmetric topography of the Alaska range along the strike-slip Denali fault: Strain partitioning and lithospheric control across a terrane suture zone. *Tectonics*, *33*(8), 1519–1533.

Fuis, G. S., Moore, T. E., Plafker, G., Brocher, T. M., Fisher, M. A., Mooney, W. D., et al. (2008). Trans-Alaska Crustal Transect and continental evolution involving subduction underplating and synchronous foreland thrusting. *Geology*, *36*(3), 267–270.

Gama, I., Fischer, K. M., Dalton, C. A., & Eilon, Z. (2022). Variations in lithospheric thickness across the Denali fault and in northern Alaska. *Geophysical Research Letters*, e2022GL101256.

Garver, J. I., & Davidson, C. M. (2015). Southwestern Laurentian zircons in upper Cretaceous flysch of the Chugach-Prince William terrane in Alaska. *American Journal of Science*, *315*(6), 537–556.

George, S. W., Perez, N. D., Struble, W., Curry, M. E., & Horton, B. K. (2022). Aseismic ridge subduction focused late Cenozoic exhumation above the Peruvian flat slab. *Earth and Planetary Science Letters*, *600*, 117754.

Gianni, G. M., & Luján, S. P. (2021). Geodynamic controls on magmatic arc migration and quiescence. *Earth-Science Reviews*, *218*, 103676.

Gillis, R. J., Herriott, M. A., LePain, T. M., Benowitz, D. L., Wypych, J. A., Donelick, A., et al. (2022). *$^{40}Ar/^{39}Ar$ and U-Pb geochronology of Cretaceous-Paleocene igneous rocks and Cenozoic strata of northwestern Cook Inlet, Alaska: Linkages between arc magmatism, cooling, faulting, and forearc subsidence*. Alaska Division of Geological & Geophysical Surveys.

Glazner, A. F. (2022). Cenozoic magmatism and plate tectonics in western North America: Have we got it wrong? In G. R. Foulger, L. C. Hamilton, D. M. Jurdy, C. A. Stein, K. A. Howard, & S. Stein (Eds.), Geological Society of America Special Paper 553*In the footsteps of Warren B. Hamilton: New ideas in Earth Science* (pp. 95–108). Boulder, CO, USA: The Geological Society of America.

Gómez-Vasconcelos, M. G., Macías, J. L., Avellán, D. R., Sosa-Ceballos, G., Garduño-Monroy, V. H., Cisneros-Máximo, G., et al. (2020). The control of preexisting faults on the distribution, morphology, and volume of monogenetic volcanism in the Michoacán-Guanajuato Volcanic Field. *GSA Bulletin*, *132*(11–12), 2455–2474.

Grow, J. A., & Atwater, T. (1970). Mid-tertiary tectonic transition in the Aleutian Arc. *Geological Society of America Bulletin*, *81*(12), 3715. https://doi.org/10.1130/0016-7606(1970)81[3715:MTTITA]2.0.CO;2

Gutscher, M.-A., Olivet, J.-L., Aslanian, D., Eissen, J.-P., & Maury, R. (1999). The "lost Inca Plateau": Cause of flat subduction beneath Peru? *Earth and Planetary Science Letters*, *171*(3), 335–341.

Hall, P. S., & Kincaid, C. (2001). Diapiric flow at subduction zones: A recipe for rapid transport. *Science*, *292*(5526), 2472–2475.

Herriott, T. M. (2014). *Geologic context, age constraints, and sedimentology of a Pleistocene volcaniclastic succession near Mount Spurr volcano, south-central Alaska*. Alaska Division of Geological & Geophysical Surveys. Report of Investigations, p. 2

Hicks, S. P., Bie, L., Rychert, C. A., Harmon, N., Goes, S., Rietbrock, A., et al. (2023). Slab to back-arc to arc: Fluid and melt pathways through the mantle wedge beneath the Lesser Antilles. *Science Advances*, *9*(5), eadd2143.

Hughes, R. A., & Pilatasig, L. F. (2002). Cretaceous and tertiary terrane accretion in the Cordillera Occidental of the Andes of Ecuador. *Tectonophysics*, *345*(1–4), 29–48.

Humphreys, E. D., & Grunder, A. L. (2022). Tectonic controls on the origin and segmentation of the Cascade Arc, USA. *Bulletin of Volcanology*, *84*(12), 1–13.

Isacks, B. L., & Barazangi, M. (1977). Geometry of Benioff zones: Lateral segmentation and downwards bending of the subducted lithosphere. In *Island Arcs, Deep Sea Trenches and Back-Arc Basins* (Vol. *1*, pp. 99–114). Washington, DC: American Geophysical Union.

Jadamec, M. A. (2016). Insights on slab-driven mantle flow from advances in three-dimensional modelling. *Journal of Geodynamics*, *100*, 51–70.

Jadamec, M. A., & Billen, M. I. (2010). Reconciling surface plate motions with rapid three-dimensional mantle flow around a slab edge. *Nature*, *465*(7296), 338–341.

Jadamec, M. A., & Billen, M. I. (2012). The role of rheology and slab shape on rapid mantle flow: Three-dimensional numerical models of the Alaska slab edge. *Journal of Geophysical Research: Solid Earth*, *117*(B2).

Jadamec, M. A., Billen, M. I., & Roeske, S. M. (2013). Three-dimensional numerical models of flat slab subduction and the Denali fault driving deformation in south-central Alaska. *Earth and Planetary Science Letters*, *376*, 29–42.

Jarrard, R. D. (1986). Relations among subduction parameters. *Reviews of Geophysics*, *24*(2), 217–284.

Jiang, C., Schmandt, B., Ward, K. M., Lin, F. C., & Worthington, L. L. (2018). Upper mantle seismic structure of Alaska from Rayleigh and S wave tomography. *Geophysical Research Letters*, *45*(19), 10–350.

Jicha, B. R., Garcia, M. O., & Wessel, P. (2018). Mid-Cenozoic Pacific plate motion change: Implications for the northwest Hawaiian Ridge and circum-Pacific. *Geology*, *46*, 939–942. https://doi.org/10.1130/G45175.1

Johnston, S. T., Jane Wynne, P., Francis, D., Hart, C. J., Enkin, R. J., & Engebretson, D. C. (1996). Yellowstone in Yukon: The late Cretaceous Carmacks group. *Geology*, *24*(11), 997–1000.

Jones, J. V., III, Todd, E., Box, S. E., Haeussler, P. J., Holm-Denoma, C. S., Karl, S. M., et al. (2021). Cretaceous to Oligocene magmatic and tectonic evolution of the western Alaska Range: Insights from U-Pb and $^{40}Ar/^{39}Ar$ geochronology. *Geosphere*, *17*(1), 118–153.

Jones, J., Caine, J., Holm-Denoma, C., Ryan, J., Benowitz, J., & Drenth, B., (2017), Unraveling the boundary between the Yukon-Tanana terrane and the parautochthonous North America in eastern Alaska. In *Geological Society of America abstracts with programs* 49(6):148.

Kay, S. M., Godoy, E., & Kurtz, A. (2005). Episodic arc migration, crustal thickening, subduction erosion, and magmatism in the south-central Andes. *Geological Society of America Bulletin*, *117*(1–2), 67–88.

van Keken, P. E., Hacker, B. R., Syracuse, E. M., & Abers, G. A. (2011). Subduction factory: 4. Depth-dependent flux of H2O from subducting slabs worldwide. *Journal of Geophysical Research: Solid Earth*, *116*(B1).

Kim, Y., Abers, G. A., Li, J., Christensen, D., Calkins, J., & Rondenay, S. (2014). Alaska Megathrust 2: Imaging the megathrust zone and Yakutat/Pacific plate interface in the Alaska subduction zone. *Journal of Geophysical Research: Solid Earth*, *119*(3), 1924–1941.

Kirsch, M., Paterson, S. R., Wobbe, F., Ardila, A. M. M., Clausen, B. L., & Alasino, P. H. (2016). Temporal histories of Cordilleran continental arcs: Testing models for magmatic episodicity. *American Mineralogist*, *101*(10), 2133–2154.

Kusky, T. M., Glass, A., & Tucker, R. (2007). Structure, Cr-chemistry, and age of the Border Ranges ultramafic-mafic complex: A suprasubduction zone ophiolite complex. In K. D. Ridgway, J. M. Trop, J. M. G. Glen, & J. M. O'Neill (Eds.), *Tectonic growth of a collisional continental margin: Crustal evolution of southern Alaska*: Geological Society of America Special Paper 431 (pp. 55–94). https://doi.org/10.1130/2007.2431(04)

Laurencin, M., Graindorge, D., Klingelhoefer, F., Marcaillou, B., & Evain, M. (2018). Influence of increasing convergence obliquity and shallow slab geometry onto tectonic deformation and seismogenic behavior along the Northern Lesser Antilles zone. *Earth and Planetary Science Letters*, *492*, 59–72.

Lease, R. O., Haeussler, P. J., & O'Sullivan, P. (2016). Changing exhumation patterns during Cenozoic growth and glaciation of the Alaska Range: Insights from detrital thermochronology and geochronology. *Tectonics*, *35*, 934–955. https://doi.org/10.1002/2015TC004067

Licht, A., Win, Z., Westerweel, J., Cogné, N., Morley, C. K., Chantraprasert, S., et al. (2020). Magmatic history of central Myanmar and implications for the evolution of the Burma Terrane. *Gondwana Research*, *87*, 303–319.

Liu, X. (2022). *Interactions between a flat slab and overriding plate: Controlling factors of subduction dynamics and continental deformation*. Dissertation.

Liu, X., & Currie, C. (2022). Origin of the Sierras Pampeanas, Argentina: Flat-slab subduction and inherited structures. *Geology*, *51*. https://doi.org/10.1130/G50551.1

Ludwig, K. R. (2012). *User's manual for Isoplot 3.75: A geochronological toolkit for Microsoft Excel*. Berkeley Geochronology Center Special Publication, 5, p. 75.

Ma, X., Attia, S., Cawood, T., Cao, W., Xu, Z., & Li, H. (2022). Arc tempos of the Gangdese batholith, southern Tibet. *Journal of Geodynamics*, *149*, 101897.

MacKenzie, L., Abers, G. A., Fischer, K. M., Syracuse, E. M., Protti, J. M., Gonzalez, V., & Strauch, W. (2008). Crustal structure along the southern Central American volcanic front. *Geochemistry, Geophysics, Geosystems*, *9*(8).

Madsen, J. K., Thorkelson, D. J., Friedman, R. M., & Marshall, D. D. (2006). Cenozoic to Recent plate configurations in the Pacific Basin: Ridge subduction and slab window magmatism in western North America. *Geosphere*, *2*(1), 11–34.

Manea, V., & Gurnis, M. (2007). Subduction zone evolution and low viscosity wedges and channels. *Earth and Planetary Science Letters*, *264*(1–2), 22–45.

Manea, V. C., Pérez-Gussinyé, M., & Manea, M. (2012). Chilean flat slab subduction controlled by overriding plate thickness and trench rollback. *Geology*, *40*(1), 35–38.

Mann, M. E., Abers, G. A., Daly, K., & Christensen, D. H. (2022). Subduction of an oceanic plateau across southcentral Alaska: Scattered-wave imaging. *Journal of Geophysical Research: Solid Earth*, e2021JB022697.

Mann, M., Fischer, K., & Benowitz, J. (2024). *Insights into inherited crustal features and southern Alaska tectonic history from Sp receiver functions, Tectonics and Seismicity of Alaska and Northwestern Canada: EarthScope and Beyond*. American Geophysical Union, Wiley.

Manselle, P., Brueseke, M. E., Trop, J. M., Benowitz, J. A., Snyder, D. C., & Hart, W. K. (2020). Geochemical and stratigraphic analysis of the Chisana Formation, Wrangellia terrane, eastern Alaska: Insights into Early Cretaceous magmatism and tectonics along the northern Cordilleran margin. *Tectonics*, *39*(8), e2020TC006131.

Marot, M., Monfret, T., Gerbault, M., Nolet, G., Ranalli, G., & Pardo, M. (2014). Flat versus normal subduction zones: A comparison based on 3-D regional traveltime tomography and petrological modelling of central Chile and western Argentina (29–35 S). *Geophysical Journal International*, *199*(3), 1633–1654.

Mathieu, L., van Wyk de Vries, B., Pilato, M., & Troll, V. R. (2011). The interaction between volcanoes and strike-slip transtensional and transpressional fault zones: Analogue models and natural ex-amples. *Journal of Structural Geology*, *33*, 898–906. https://doi.org/10.1016/j.jsg.2011.03.0003

McClelland, W. C., Strauss, J. V., Colpron, M., Gilotti, J. A., Faehnrich, K., Malone, S. J., et al. (2021). 'Taters versus sliders: Evidence for a long-lived history of strike-slip displacement along the Canadian Arctic transform system (CATS). *GSA Today*, *31*(7), 4–11. https://doi.org/10.1130/GSATG500A.1

McConeghy, J., Flesch, L., & Elliott, J. (2022). Investigating the effect of mantle flow and viscosity structure on surface velocities in Alaska using 3-D geodynamic models. *Journal of Geophysical Research: Solid Earth*, *127*(10), e2022JB024704.

Miller, M. L., Bradley, D. C., Bundtzen, T. K., & McClelland, W. (2002). Late cretaceous through Cenozoic strike-slip tectonics of southwestern Alaska. *The Journal of Geology*, *110*(3), 247–270.

Miller, M. S., O'Driscoll, L. J., Porritt, R. W., & Roeske, S. M. (2018). Multiscale crustal architecture of Alaska inferred from P receiver functions. *Lithosphere*, *10*(2), 267–278.

Newell, D. L., Benowitz, J. A., Regan, S. P., & Hiett, C. D. (2023). Roadblocks and speed limits: Mantle-to-surface volatile flux through the lithospheric-scale Denali fault, Alaska. *Geology*, *51*(6), 576–580.

O'Driscoll, L. J., Humphreys, E. D., & Saucier, F. (2009). Subduction adjacent to deep continental roots: Enhanced negative pressure in the mantle wedge, mountain building and continental motion. *Earth and Planetary Science Letters*, *280*(1–4), 61–70.

O'Driscoll, L. J., & Miller, M. S. (2015). Lithospheric discontinuity structure in Alaska, thickness variations determined by Sp receiver functions. *Tectonics*, *34*(4), 694–714.

Panuska, B. C., Stone, D. B., & Turner, D. L. (1990). Paleomagnetism of eocene volcanic rocks, Talkeetna Mountains, Alaska. *Journal of Geophysical Research: Solid Earth*, *95*(B5), 6737–6750.

Pavlis, T. L., Amato, J. M., Trop, J. M., Ridgway, K. D., Roeske, S. M., & Gehrels, G. E. (2019). Subduction polarity in ancient arcs: A call to integrate geology and geophysics to decipher the Mesozoic tectonic history of the Northern Cordillera of North America. *GSA Today*, *29*(11), 4–10.

Pavlis, G., Jadamec, M., Mann, M. E., Yang, X., Schaeffer, A., Wei, S., & Fischer, K. (2024). *Synthesis of the seismic structure of the Greater Alaska Region: Subducting slab geometry. Tectonics and Seismicity of Alaska and Northwestern Canada: EarthScope and Beyond*. American Geophysical Union, Wiley.

Porter, R., & Reid, M. (2021). Mapping the thermal lithosphere and melting across the continental US. *Geophysical Research Letters*, *48*(7), e2020GL092197.

Rabiee, A., Rossetti, F., Asahara, Y., Azizi, H., Lucci, F., Lustrino, M., & Nozaem, R. (2020). Long-lived, Eocene-Miocene stationary magmatism in NW Iran along a transform plate boundary. *Gondwana Research*, *85*, 237–262.

Regan, S. P., Benowitz, J. A., & Holland, M. E. (2020). A plutonic brother from another magma mother: Disproving the Eocene Foraker-McGonagall pluton piercing point and implications for long-term slip on the Denali fault. *Terra Nova*, *32*(1), 66–74.

Regan, S. P., Benowitz, J. A., Waldien, T. S., Holland, M. E., Roeske, S. M., O'Sullivan, P., & Layer, P. (2021). Long distance plutonic relationships demonstrate 33 million years of strain partitioning along the Denali fault. *Terra Nova*, *33*(6), 630–640.

Richards, J. P. (2003). Tectono-magmatic precursors for porphyry Cu-(Mo-Au) deposit formation. *Economic Geology*, *98*(8), 1515–1533.

Richards, M. A., & Lithgow-Bertelloni, C. (1996). Plate motion changes, the Hawaiian-Emperor bend, and the apparent success and failure of geodynamic models. *Earth and Planetary Science Letters*, *137*(1–4), 19–27. https://doi.org/10.1016/0012-821X(95)00209-U

Richter, D. H., Smith, J. G., Lanphere, M. A., Dalrymple, G. B., Reed, B. L., & Shew, N. (1990). Age and progression of volcanism, Wrangell volcanic field, Alaska. *Bulletin of Volcanology*, *53*(1), 29–44.

Ridgway, K. D., Trop, J. M., Nokleberg, W. J., Davidson, C. M., & Eastham, K. R. (2002). Mesozoic and Cenozoic tectonics of the eastern and central Alaska Range: Progressive basin development and deformation in a suture zone. *Geological Society of America Bulletin*, *114*(12), 1480–1504.

Rodríguez-González, J., Billen, M. I., & Negredo, A. M. (2014). Non-steady-state subduction and trench-parallel flow induced by overriding plate structure. *Earth and Planetary Science Letters*, *401*, 227–235.

Rodríguez-González, J., Negredo, A. M., & Billen, M. I. (2012). The role of the overriding plate thermal state on slab dip variability and on the occurrence of flat subduction. *Geochemistry, Geophysics, Geosystems*, *13*(1).

Rondenay, S., Montési, L. G., & Abers, G. A. (2010). New geophysical insight into the origin of the Denali volcanic gap. *Geophysical Journal International*, *182*(2), 613–630.

Rosenthal, J., Fitzgerald, P., Benowitz, J., & Metcalf, J. (2024). *Slip redistribution onto the preferentially aligned Totschunda Fault of Southern Alaska—A result of a relative pacific plate motion change at ca. 6 Ma, submitted to tectonics and seismicity of Alaska and Northwestern Canada: EarthScope and Beyond*. American Geophysical Union, Wiley.

Rossi, G., Abers, G. A., Rondenay, S., & Christensen, D. H. (2006). Unusual mantle Poisson's ratio, subduction, and crustal structure in central Alaska. *Journal of Geophysical Research: Solid Earth*, *111*(B9).

Saltus, R. W., & Hudson, T. L. (2022). There is more Wrangellia—magnetic characterization of southern Alaska crust. *Canadian Journal of Earth Sciences*, *59*(4), 243–257.

Saltus, R. W., Gough, L. P., & Day, W. C. (2007). Matching magnetic trends and patterns across the Tintina Fault, Alaska and Canada: Evidence for offset of about 490 kilometers. In *Recent US Geological Survey Studies in the Tintina Gold Province, Alaska, United States, and Yukon, Canada. Results of a 5-year project*.

Schaeffer, A. J., & Lebedev, S. (2014). Imaging the North American continent using waveform inversion of global and US Array data. *Earth and Planetary Science Letters*, *402*, 26–41.

Sharp, W. D., & Clague, D. A. (2006). 50-Ma initiation of Hawaiian-Emperor bend records major change in Pacific plate motion. *Science*, *313*(5791), 1281–1284.

Sharples, W., Jadamec, M. A., Moresi, L. N., & Capitanio, F. A. (2014). Overriding plate controls on subduction evolution. *Journal of Geophysical Research - Solid Earth*, *119*, 6684–6704. https://doi.org/10.1002/2014JB011163

Skinner, S. M., & Clayton, R. W. (2013). The lack of correlation between flat slabs and bathymetric impactors in South America. *Earth and Planetary Science Letters*, *371*, 1–5.

Smart, K. J., Pavlis, T. L., Sisson, V. B., Roeske, S. M., & Snee, L. W. (1996). The Border Ranges fault system in Glacier Bay National Park, Alaska: Evidence for major early Cenozoic dextral strike-slip motion. *Canadian Journal of Earth Sciences*, *33*(9), 1268–1282.

Stamatakos, J. A., Trop, J. M., & Ridgway, K. D. (2001). Late Cretaceous paleogeography of Wrangellia: Paleomagnetism of the MacColl Ridge Formation, southern Alaska, revisited. *Geology*, *29*(10), 947–950.

Stern, C. R. (2011). Subduction erosion: Rates, mechanisms, and its role in arc magmatism and the evolution of the continental crust and mantle. *Gondwana Research*, *20*(2–3), 284–308.

Stevenson, D. J., & Turner, J. S. (1977). Angle of subduction. *Nature*, *270*(5635), 334–336.

Stock, J., & Molnar, P. (1988). Uncertainties and implications of the Late Cretaceous and Tertiary position of North America relative to the Farallon, Kula, and Pacific Plates. *Tectonics*, *7*(6), 1339–1384. https://doi.org/10.1029/TC007i006p01339

Sykes, L. R. (1978). Intraplate seismicity, reactivation of preexisting zones of weakness, alkaline magmatism, and other tectonism postdating continental fragmentation. *Reviews of Geophysics*, *16*(4), 621–688.

Syracuse, E. M., & Abers, G. A. (2006). Global compilation of variations in slab depth beneath arc volcanoes and implications: ARC VOLCANO SLAB DEPTH. *Geochemistry, Geophysics, Geosystems*, *7*(5). https://doi.org/10.1029/2005GC001045

Taramón, J. M., Rodríguez-González, J., Negredo, A. M., & Billen, M. I. (2015). Influence of cratonic lithosphere on the formation and evolution of flat slabs: Insights from 3-D time-dependent modeling. *Geochemistry, Geophysics, Geosystems*, *16*(9), 2933–2948.

Terhune, P. J., Benowitz, J. A., Trop, J. M., O'Sullivan, P. B., Gillis, R. J., & Freymueller, J. T. (2019). Cenozoic tectono-thermal history of the southern Talkeetna Mountains, Alaska: Insights into a potentially alternating convergent and transform plate margin. *Geosphere*, *15*(5), 1539–1576.

Tibaldi, A., Bonali, F. L., & Corazzato, C. (2017). Structural control on volcanoes and magma paths from local-to orogen-scale: The central Andes case. *Tectonophysics*, *699*, 16–41.

Tikoff, B., Housen, B. A., Maxson, J. A., Nelson, E. M., Trevino, S., & Shipley, T. F. (2023). Hit- and-run model for Cretaceous–Paleogene tectonism along the western margin of Laurentia. In *Laurentia: Turning Points in the Evolution of a Continent* (Vol. *220*). Geological Society of America Memoir.

Tovish, A., Schubert, G., & Luyendyk, B. P. (1978). Mantle flow pressure and the angle of subduction: Non-Newtonian corner flows. *Journal of Geophysical Research: Solid Earth*, *83*(B12), 5892–5898.

Trop, J. M., Benowitz, J., Cole, R. B., & O'Sullivan, P. (2019). Cretaceous to Miocene magmatism, sedimentation, and exhumation within the Alaska Range suture zone: A polyphase reactivated terrane boundary. *Geosphere*, *15*(4), 1066–1101.

Trop, J. M., Benowitz, J. A., Kirby, C. S., & Brueseke, M. E. (2022). Geochronology of the Wrangell Arc: Spatial-temporal evolution of slab-edge magmatism along a flat-slab, subduction-transform transition, Alaska-Yukon. *Geosphere*, *18*(1), 19–48.

Trop, J. M., Benowitz, J. A., Koepp, D. Q., Sunderlin, D., Brueseke, M. E., Layer, P. W., & Fitzgerald, P. G. (2020). Stitch in the ditch: Nutzotin Mountains (Alaska) fluvial strata and a dike record ca. 117–114 Ma accretion of Wrangellia with western North America and initiation of the Totschunda fault. *Geosphere*, *16*(1), 82–110.

Trop, J. M., Hart, W. K., Snyder, D., & Idleman, B. (2012). Miocene basin development and volcanism along a strike-slip to flat-slab subduction transition: Stratigraphy, geochemistry, and geochronology of the central Wrangell volcanic belt, Yakutat–North America collision zone. *Geosphere*, *8*(4), 805–834.

Trop, J. M., & Ridgway, K. D. (2007). Mesozoic and Cenozoic tectonic growth of southern Alaska: A sedimentary basin perspective. In K. D. Ridgway, J. M. Trop, J. M. G. Glen, & J. M. O'Neill (Eds.), *Tectonic growth of a collisional continental margin: Crustal evolution of southern Alaska*: Geological Society of America Special Paper 431 (pp. 55–94). https://doi.org/10.1130/2007.2431(04)

Van Hunen, J., van den Berg, A. P., & Vlaar, N. J. (2004). Various mechanisms to induce present-day shallow flat subduction and implications for the younger Earth: A numerical parameter study. *Physics of the Earth and Planetary Interiors*, *146*(1–2), 179–194.

Van Hunen, J., van den Berg, A. P., & Vlaar, N. J. (2002). On the role of subducting oceanic plateaus in the development of shallow flat subduction. *Tectonophysics*, *352*(3–4), 317–333.

Vauchez, A., Tommasi, A., & Mainprice, D. (2012). Faults (shear zones) in the Earth's mantle. *Tectonophysics*, *558*, 1–27.

Veenstra, E., Christensen, D. H., Abers, G. A., & Ferris, A. (2006). Crustal thickness variation in south-central Alaska. *Geology*, *34*(9), 781–784.

Waldien, T. S., Roeske, S. M., & Benowitz, J. A. (2021). Tectonic underplating and dismemberment of the Maclaren-Kluane Schist records late cretaceous terrane accretion polarity and ~480 km of post-52 Ma dextral displacement on the Denali fault. *Tectonics*, *40*(10).

Webb, M., White, L. T., Jost, B. M., Tiranda, H., & BouDagher-Fadel, M. (2020). The history of Cenozoic magmatism and collision in NW New Guinea-New insights into the tectonic evolution of the northernmost margin of the Australian Plate. *Gondwana Research*, *82*, 12–38. https://doi.org/10.1016/j.gr.2019.12.0100

Wells, R., Bukry, D., Friedman, R., Pyle, D., Duncan, R., Haeussler, P., & Wooden, J. (2014). Geologic history of Siletzia, a large igneous province in the Oregon and Washington Coast Range: Correlation to the geomagnetic polarity time scale and implications for a long-lived Yellowstone hotspot. *Geosphere*, *10*(4), 692–719.

Westerweel, J., Roperch, P., Licht, A., Dupont-Nivet, G., Win, Z., Poblete, F., et al. (2019). Burma Terrane part of the Trans-Tethyan arc during collision with India according to palaeomagnetic data. *Nature Geoscience*, *12*(10), 863–868.

Wilson, F. H., Hults, C. P., Mull, C. G., & Karl, S. M. (2015). *Geologic map of Alaska*. US Department of the Interior, US Geological Survey.

Wilson, C. R., Spiegelman, M., van Keken, P. E., & Hacker, B. R. (2014). Fluid flow in subduction zones: The role of solid rheology and compaction pressure. *Earth and Planetary Science Letters*, *401*, 261–274. https://doi.org/10.1016/j.epsl.2014.05.052

Worthington, L. L., Van Avendonk, H. J., Gulick, S. P., Christeson, G. L., & Pavlis, T. L. (2012). Crustal structure of the Yakutat terrane and the evolution of subduction and collision in southern Alaska. *Journal of Geophysical Research: Solid Earth*, *117*(B1).

Yang, G., Li, Y., Xiao, W., & Tong, L. (2015). OIB-type rocks within West Junggar ophiolitic mélanges: Evidence for the accretion of seamounts. *Earth-Science Reviews*, *150*, 477–496. https://doi.org/10.1016/j.earscirev.2015.09.002

Yang, X., Mann, M. E., Fischer, K., Jadamec, M., Wei, S. S., Pavlis, G., & Schaeffer, A. (2024). *Synthesis of the seismic structure of the greater Alaska Region: Continental lithosphere. Tectonics and Seismicity of Alaska and Northwestern Canada: EarthScope and Beyond*. American Geophysical Union, Wiley.

Yuan, H., & Romanowicz, B. (2010). Lithospheric layering in the North American craton. *Nature*, *466*(7310), 1063–1068.

Zhang, Z., Zack, T., Kohn, B., Malusà, M. G., Wu, L., Rezaeian, M., et al. (2023). From Tethyan subduction to Arabia-Eurasia continental collision: Multiple geo-thermochronological signals from granitoids in NW Iran. *Palaeogeography, Palaeoclimatology, Palaeoecology*, *621*, 111567.